Gravitational wave evolution from acoustic and vortical sources

- Pencil Code
- Correspondence between kinetic or magnetic spectra with GW spectra
- Inertial and subinertial range spectra
- Scalar and vector modes in vertical and acoustic (irrotational) turbulence
- Onset of GW energy and vorticity

Axel Brandenburg, Tina Kahniashvili, Arthur Kosowsky, Sayan Mandal, & Alberto Roper Pol

Small Lorentz factors, γ~1

$$
\begin{aligned}
\frac{\partial \ln \rho}{\partial t} &= -\frac{4}{3}\left(\boldsymbol{\nabla}\cdot\boldsymbol{u} + \boldsymbol{u}\cdot\boldsymbol{\nabla}\ln\rho\right) \\
&\quad + \frac{1}{\rho}\left[\boldsymbol{u}\cdot(\boldsymbol{J}\times\boldsymbol{B}) + \eta\boldsymbol{J}^2\right], \\
\frac{\partial \boldsymbol{u}}{\partial t} &= -\boldsymbol{u}\cdot\boldsymbol{\nabla}\boldsymbol{u} + \frac{\boldsymbol{u}}{3}\left(\boldsymbol{\nabla}\cdot\boldsymbol{u} + \boldsymbol{u}\cdot\boldsymbol{\nabla}\ln\rho\right) \\
&\quad - \frac{\boldsymbol{u}}{\rho}\left[\boldsymbol{u}\cdot(\boldsymbol{J}\times\boldsymbol{B}) + \eta\boldsymbol{J}^2\right] - \frac{1}{4}\boldsymbol{\nabla}\ln\rho \\
&\quad + \frac{3}{4\rho}\boldsymbol{J}\times\boldsymbol{B} + \frac{2}{\rho}\boldsymbol{\nabla}\cdot(\rho\nu\mathsf{S}) + \boldsymbol{\mathcal{F}}, \\
\frac{\partial \boldsymbol{B}}{\partial t} &= \nabla\times\left(\boldsymbol{u}\times\boldsymbol{B} - \eta\boldsymbol{J} + \boldsymbol{\mathcal{E}}\right),
\end{aligned}
$$

Treatment in Pencil Code

Scale factor a → $\tilde{h}_{ij} = a h_{ij}$ …but then drop tilde

$$\left(\partial_{\bar{t}}^2 - c^2\nabla^2\right) h_{ij}(\boldsymbol{x},\bar{t}) = 6\,T_{ij}^{\mathrm{TT}}(\boldsymbol{x},\bar{t})/\bar{t}$$

- No damping
  - Except of the source
- Kolmogorov
- GW spectrum by k^2 steeper
- hdot not kh (=dashed)

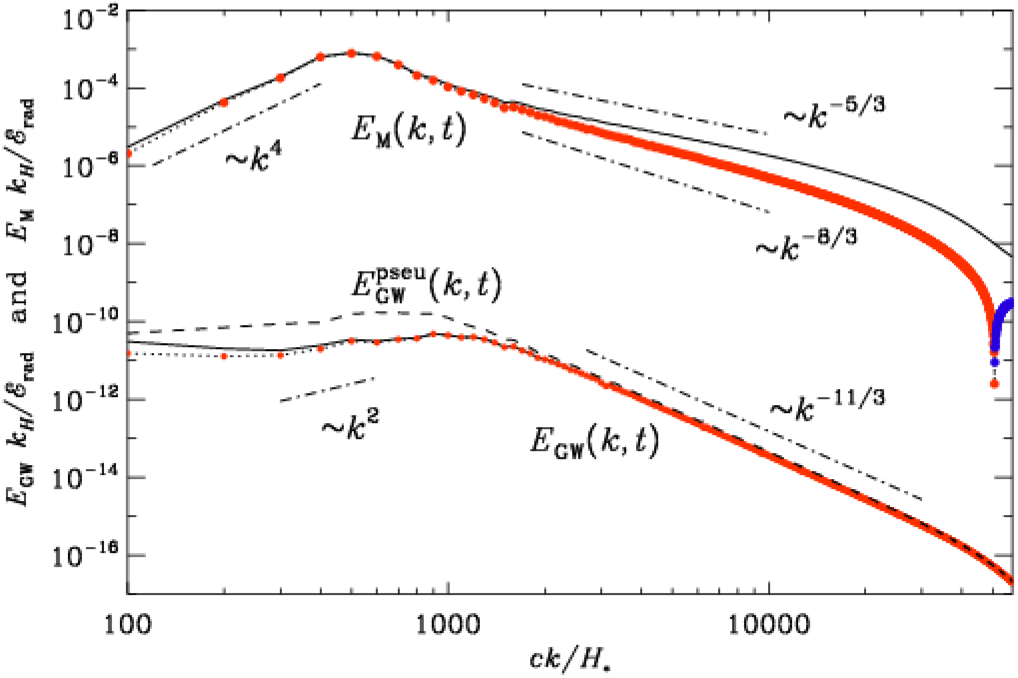

"Usual" 3rd order Runge-Kutta

$$\begin{pmatrix} h_{ij} \\ h'_{ij} \end{pmatrix}_{t+\delta t} \equiv \boldsymbol{q}_i, \quad \text{where} \quad \boldsymbol{q}_i = \boldsymbol{q}_{i-1} + \beta_i \boldsymbol{w}_i, \quad \boldsymbol{w}_i = \alpha_i \boldsymbol{w}_{i-1} + \delta t \boldsymbol{Q}_{i-1}, \quad \text{(approach I)}.$$

with $\alpha_1 = 0$, $\alpha_2 = -5/9$, $\alpha_3 = -153/128$, $\beta_1 = 1/3$, $\beta_2 = 15/16$, $\beta_3 = 8/15$, and

$$\boldsymbol{q}_{i-1} \equiv \begin{pmatrix} h_{ij} \\ h'_{ij} \end{pmatrix}_t, \quad \boldsymbol{Q}_{i-1} \equiv \begin{pmatrix} h'_{ij} \\ c^2 \nabla^2 h_{ij} + \mathcal{G} T_{ij} \end{pmatrix}_t.$$

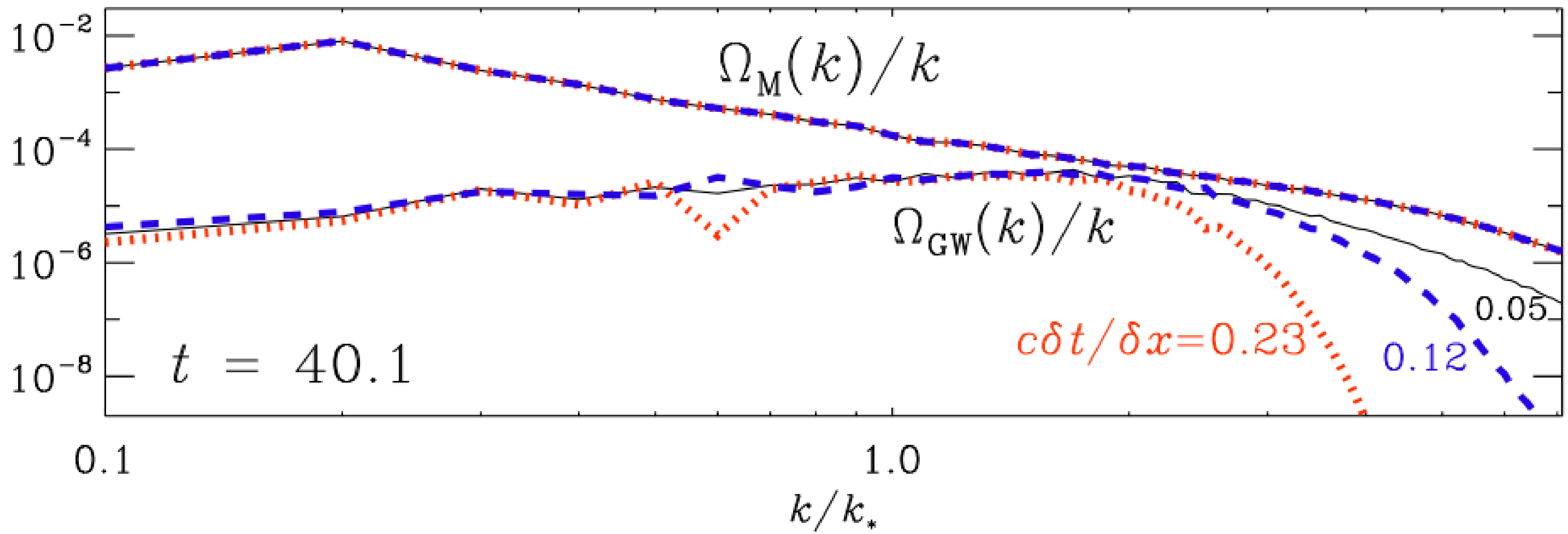

"Exact" between 2 time steps

$$\begin{pmatrix} \omega\tilde{h} - \omega^{-1}\mathcal{G}\tilde{T} \\ \tilde{h}' \end{pmatrix}_{+,\times}^{t+\delta t} = \begin{pmatrix} \cos\omega\delta t & \sin\omega\delta t \\ -\sin\omega\delta t & \cos\omega\delta t \end{pmatrix} \begin{pmatrix} \omega\tilde{h} - \omega^{-1}\mathcal{G}\tilde{T} \\ \tilde{h}' \end{pmatrix}_{+,\times}^{t}$$

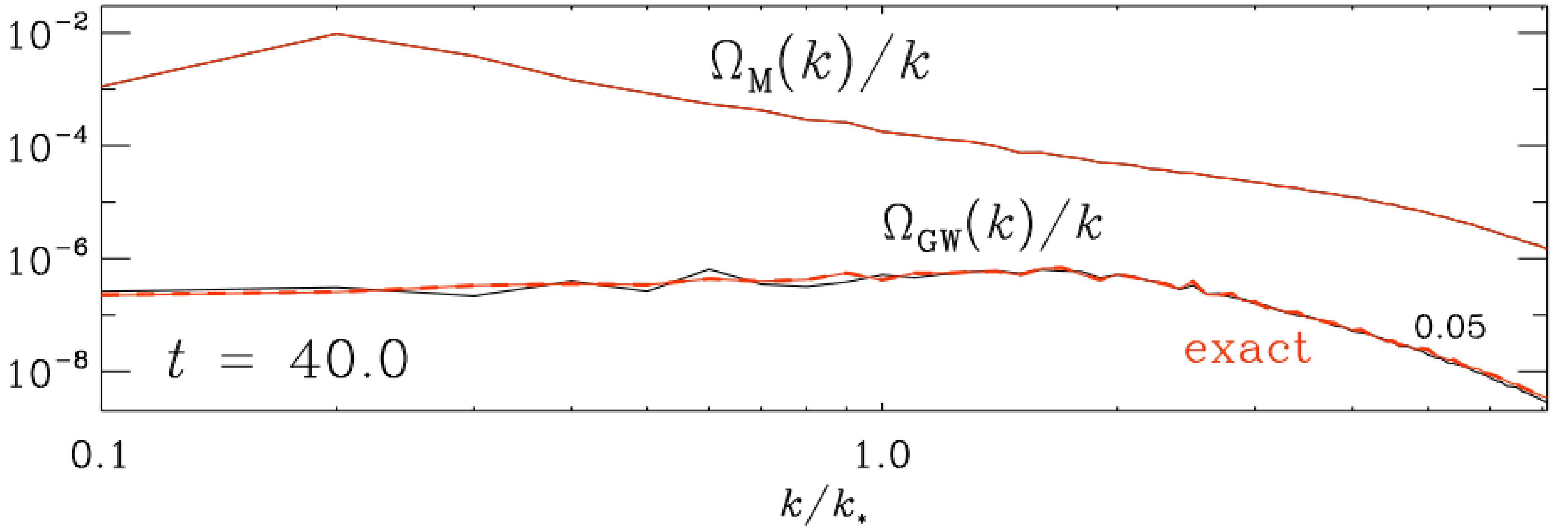

Pencil Code

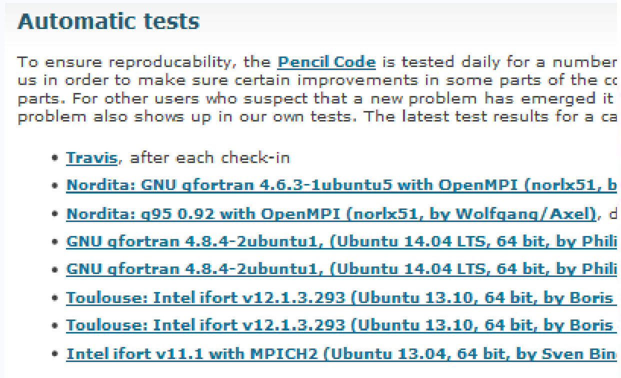

Repositories 4 | Packages | People 77 | Teams

- 2001 – 2007: cvs at Nordita (w/Dobler)
- 2007 – 2008: svn at Nordita (+Heinemann)
- 2008 – 2015: svn on google code
- 2015 – now: svn & git on github
  - CUDA, particle & various other modules
  - PCSC → Pencil Code Steering Committee

Now 30,218 commits

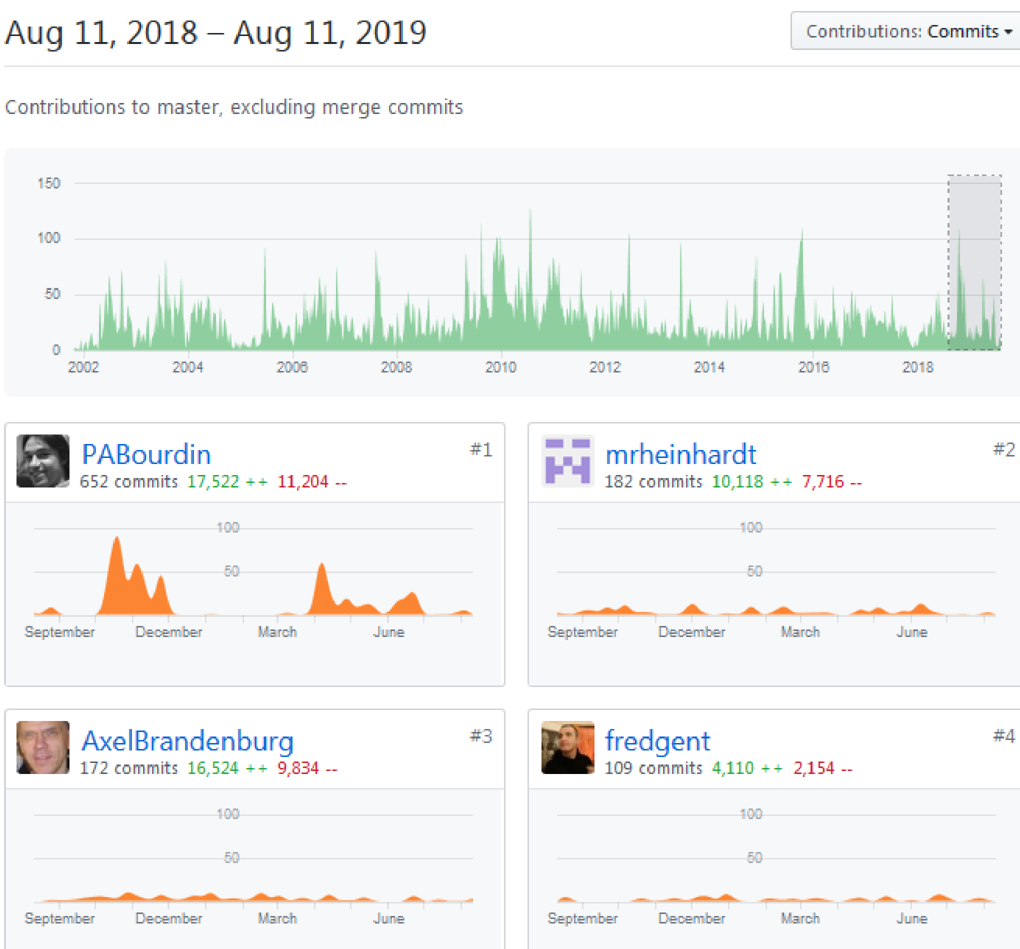

H-index = 34, i.e.,

34 people did >34 commits

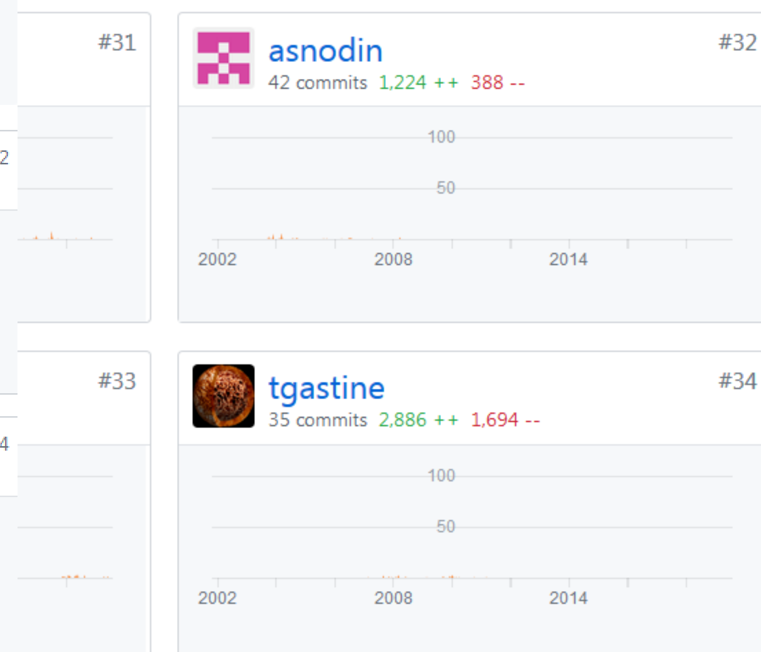

Updates since last year

A search using `http://adslabs.org` or Bumblebee `https://ui.adsabs.harvard.edu/` lists the papers in which the Pencil Code is being quoted. In the following we present the papers that are making use of the code either for their own scientific work of those authors, or for code comparison purposes. We include conference proceedings, which make up 15–20% of all papers. We classify the references by year and by topic, although the topics are often overlapping. The primary application of the Pencil Code lies in astrophysics, in which case we classify mostly by the field of research.

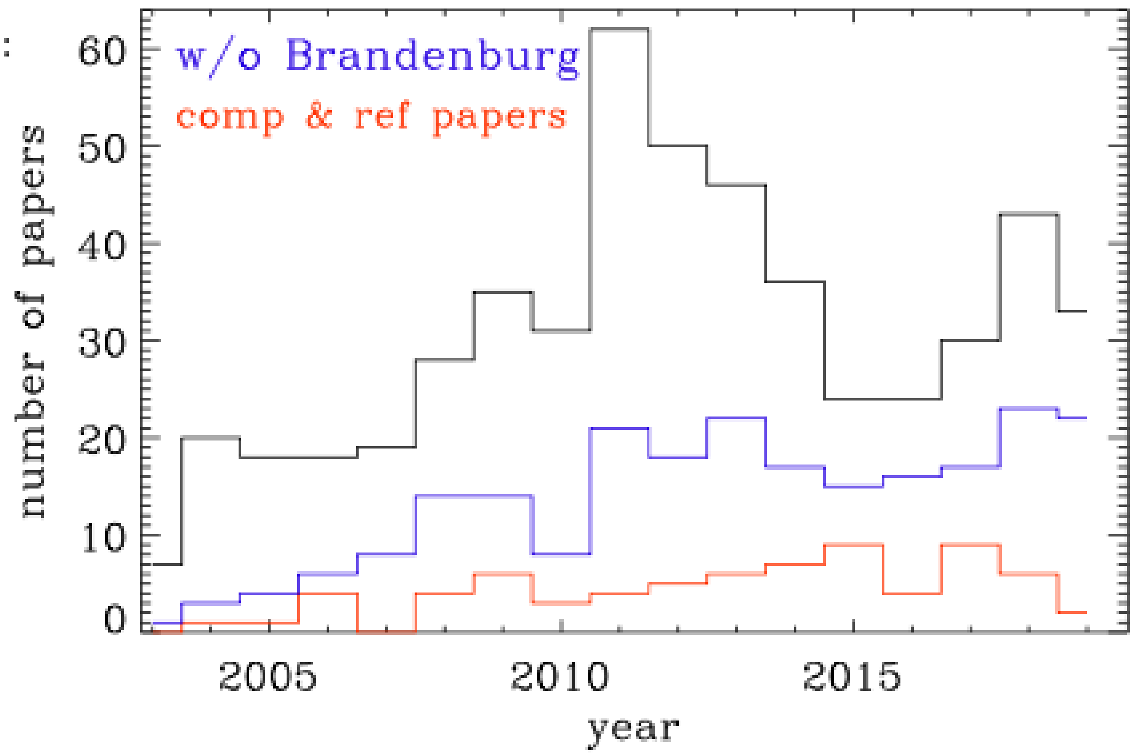

Figure 1: Number of papers since 2003 that make use of the Pencil Code. In red is shown the number of papers that reference it for code comparison or other purposes and in blue the papers that are not co-authored by Brandenburg. The enhanced number of papers during 2011–2013 results from publications related to his ERC Advanced Grant.

Special Issue

Special issue on ``Physics and Algorithms of the Pencil Code'' in Geophysical & Astrophysical Fluid Dynamics (GAFD)

0) Editorial (PDF, 5 pages)

http://norlx51.nordita.org/~brandenb/tmp/editorial/paper.pdf

1) Käpylä, P. J., Gent, F. A., Olspert, N., Käpylä, M. J., & Brandenburg, A.: 2019, ``Sensitivity to luminosity, centrifugal force, and boundar conditions in spherical shell convection,'' *Geophys. Astrophys. Fluid Dyn.* (arXiv: 1807.09309, DOI: 10.1080/03091929.2019.1571586, PDF, 25 pages)

2) Aarnes, J. R., Jin, T., Mao, C., Haugen, N. E. L., Luo, K., Andersson, H. I.: , 2018, ``Treatment of solid objects in the Pencil Code using an immersed boundary method and overset grids ,'' *Geophys. Astrophys. Fluid Dyn.*, published (arXiv: 1806.06776, DOI: 10.1080/03091929.2018.1492720, PDF, 23 pages)

3) Qian, C., Wang, C., Liu, J., Brandenburg, A., Haugen, N. E. L., & Liberman, M.: 2019, ``Convergence properties of detonation simulations,'' *Geophys. Astrophys. Fluid Dyn.*, in press (arXiv: 1902.03816, ADS, HTML, PDF, 17 pages)

4) Gent, F. A., Mac Low, M.-M., Kä,pylä,, M. J., Sarson, G. R., Hollins, J. F. , 2018, ``Modelling supernova driven turbulence,'' *Geophys. Astrophys. Fluid Dyn.* (arXiv: 1806.01570, DOI: 10.1080/03091929.2019.1634705, PDF, 29 pages)

5) Schober, J., Brandenburg, A., & Rogachevskii, I.: 2019, ``Chiral fermion asymmetry in high-energy plasma simulations,'' *Geophys. Astrophys. Fluid Dyn.* (arXiv: 1808.06624, ADS, DOI: 10.1080/03091929.2019.1591393, PDF, 24 pages)

6) Roper Pol, A., Brandenburg, A., Kahniashvili, T., Kosowsky, A., Mandal, S.: 2018, ``The timestep constraint in solving the gravitational wave equations sourced by hydromagnetic turbulence,'' *Geophys. Astrophys. Fluid Dyn.*, in press (arXiv: 1807.05479, DOI: 10.1080/03091929.2019.1653460, PDF, 32 pages)

7) Brandenburg, A., & Das, U.: 2019, ``The time step constraint in radiation hydrodynamics,'' *Geophys. Astrophys. Fluid Dyn.*, submitted (arXiv: 1901.06385, ADS, HTML, PDF, 29 pages)

8) Singh, N. K., Raichur, H., Käpylä, M. J., Rheinhardt, M., Brandenburg, A., & Käpylä, P. J.: 2018, ``f-mode strengthening from a localized bipolar subsurface magnetic field,'' *Geophys. Astrophys. Fluid Dyn.* (arXiv: 1808.08904, ADS, DOI: 10.1080/03091929.2019.1653461, PDF, 17 pages)

9) Chatterjee, P. , 2018, ``Testing Alfven wave propagation in a realistic set-up of the solar atmosphere,'' *Geophys. Astrophys. Fluid Dyn.*, in press (arXiv: 1806.08166, 17 pages)

10) Warnecke, J., & Bingert, S.: 2018, *Geophys. Astrophys. Fluid Dyn.*, in press (arXiv: 1811.01572, 17 pages)

11) Bourdin, P. A.: 2018, ``Driving solar coronal MHD simulations on high-performance computers,'' *Geophys. Astrophys. Fluid Dyn.* (arXiv: 1908.08557, DOI: 10.1080/03091929.2019.1643849, PDF, 26 pages)

Definition of spectra

$$E_{\mathrm{M}}(k) = \frac{1}{2} \sum_{k_- < |\boldsymbol{k}| \leqslant k_+} |\tilde{\boldsymbol{B}}(\boldsymbol{k})|^2,$$

$$H_{\mathrm{M}}(k) = \frac{1}{2} \sum_{k_- < |\boldsymbol{k}| \leqslant k_+} (\tilde{\boldsymbol{A}} \cdot \tilde{\boldsymbol{B}}^* + \tilde{\boldsymbol{A}}^* \cdot \tilde{\boldsymbol{B}}),$$

$k_\pm = k \pm \delta k/2$ and $\delta k = 2\pi/L$ is the

$$\int_0^\infty E(k)\,\mathrm{d}k = \frac{1}{2}\langle \boldsymbol{u}^2 \rangle$$

Self-similar turbulent decay

$$E_{\mathrm{M}}(k\xi_{\mathrm{M}}(t),t) \approx \xi_{\mathrm{M}}^{-\beta_{\mathrm{M}}}\phi(k\xi_{\mathrm{M}}).$$

$$\int E_i(k,t)\,\mathrm{d}k = \mathcal{E}_i \qquad \xi_i(t) = \int_0^\infty k^{-1}E_i(k,t)\,\mathrm{d}k/\mathcal{E}_i(t)$$

instantaneous $\quad p_i(t) = d\ln\mathcal{E}_i/d\ln t, \quad q_i(t) = d\ln\xi_i/d\ln t,$

scaling exponents $\quad 1+\beta_{\mathrm{M}} = p_{\mathrm{M}}/q_{\mathrm{M}}$

β	p	q	inv.	dim.
4	$10/7 \approx 1.43$	$2/7 \approx 0.286$	$\mathcal{L}$	$[x]^7[t]^{-2}$
3	$8/6 \approx 1.33$	$2/6 \approx 0.333$		
2	$6/5 = 1.20$	$2/5 = 0.400$		
1	$4/4 = 1.00$	$2/4 = 0.500$	$\langle \boldsymbol{A}_{\mathrm{2D}}^2 \rangle$	$[x]^4[t]^{-2}$
0	$2/3 \approx 0.67$	$2/3 \approx 0.667$	$\langle \boldsymbol{A}\cdot\boldsymbol{B} \rangle$	$[x]^3[t]^{-2}$
-1	$0/2 = 0.00$	$2/1 = 1.000$		

Collapsed spectra and *pq* diagrams

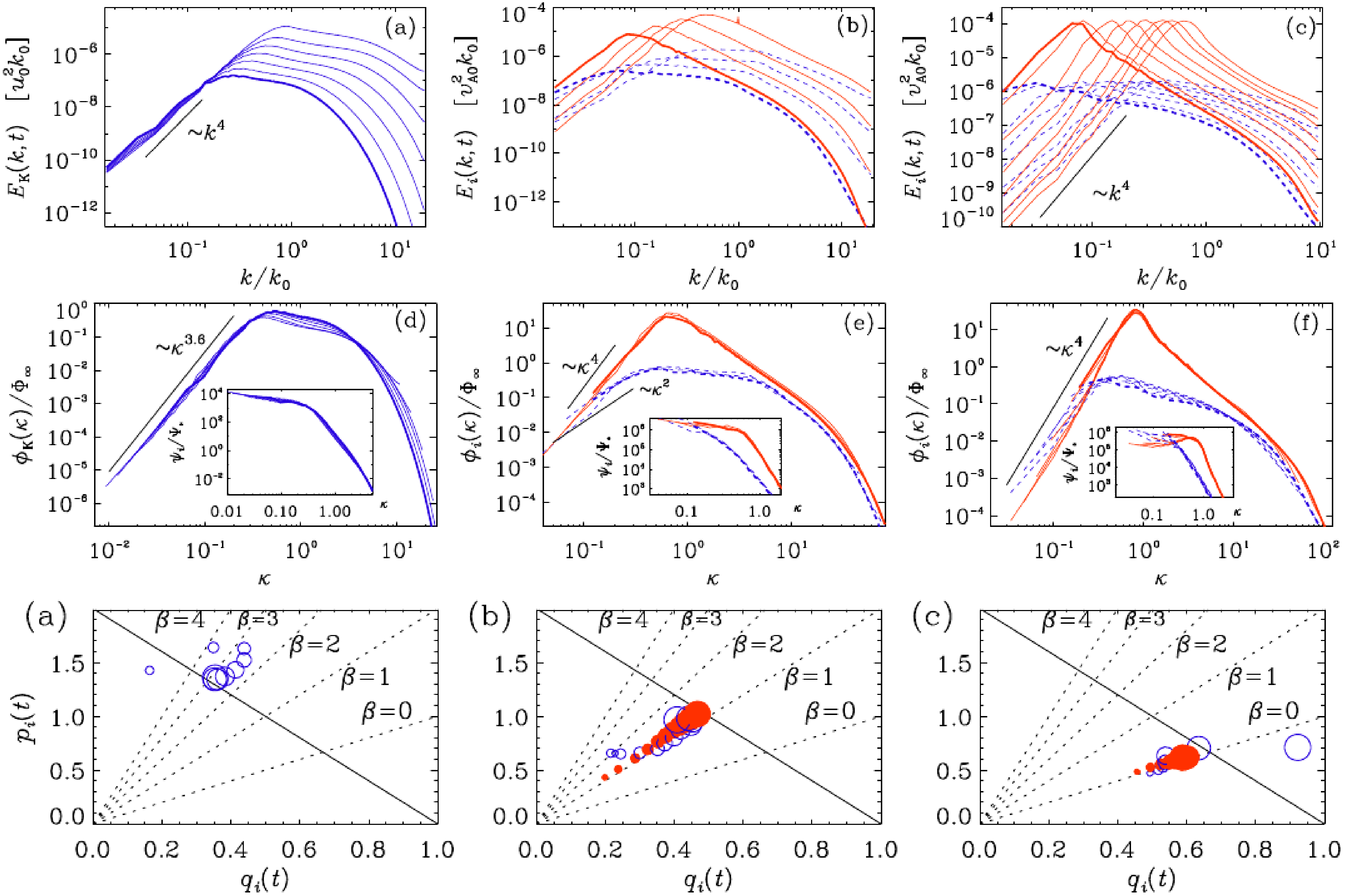

Nonhelical inverse transfer: k^{-2} spectrum

Brandenburg, Kahniashvili, & Tevzadze (PRL 114, 075001, 2015)

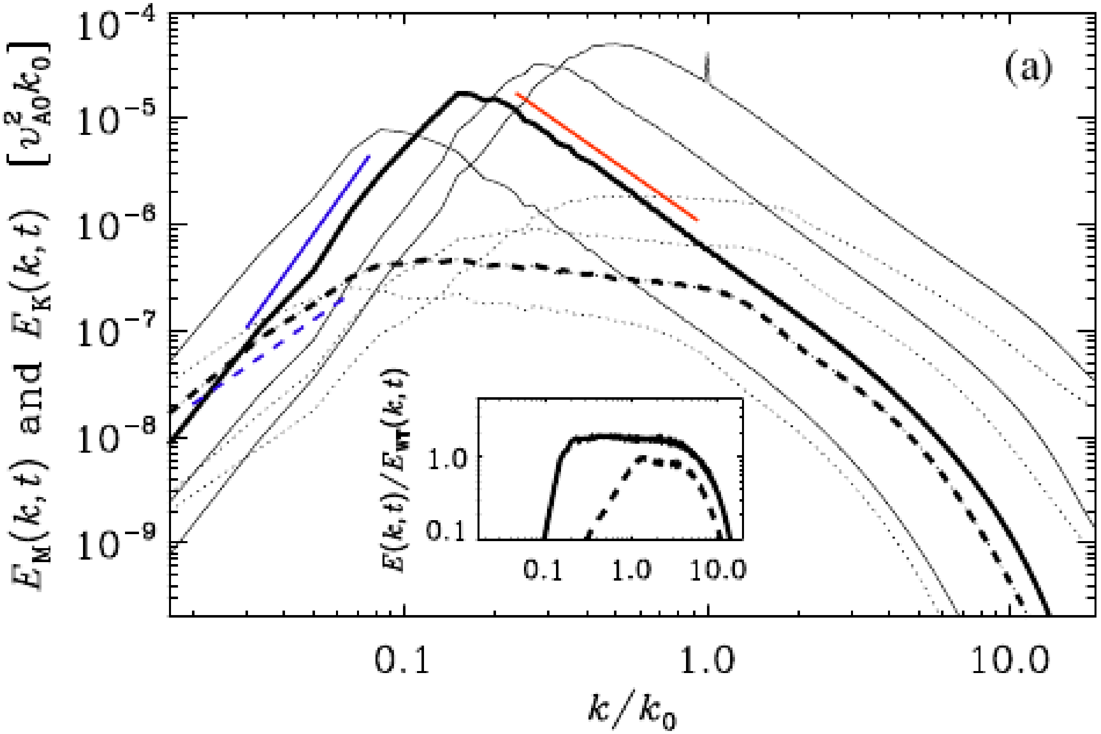

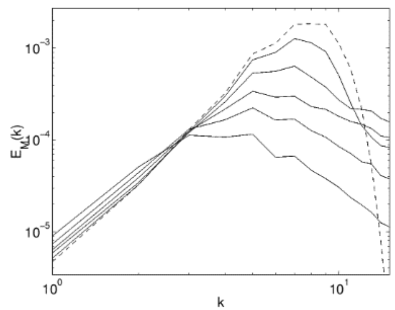

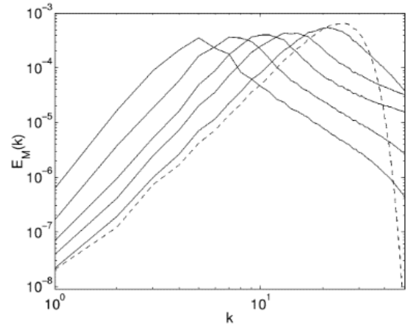

helical vs nonhelical

So-called “weak” (or wave) turbulence

$$E_{\mathrm{WT}}(k,t) = C_{\mathrm{WT}}(\epsilon v_A k_M)^{1/2} k^{-2},$$

Horizon scales for k^4 spectrum

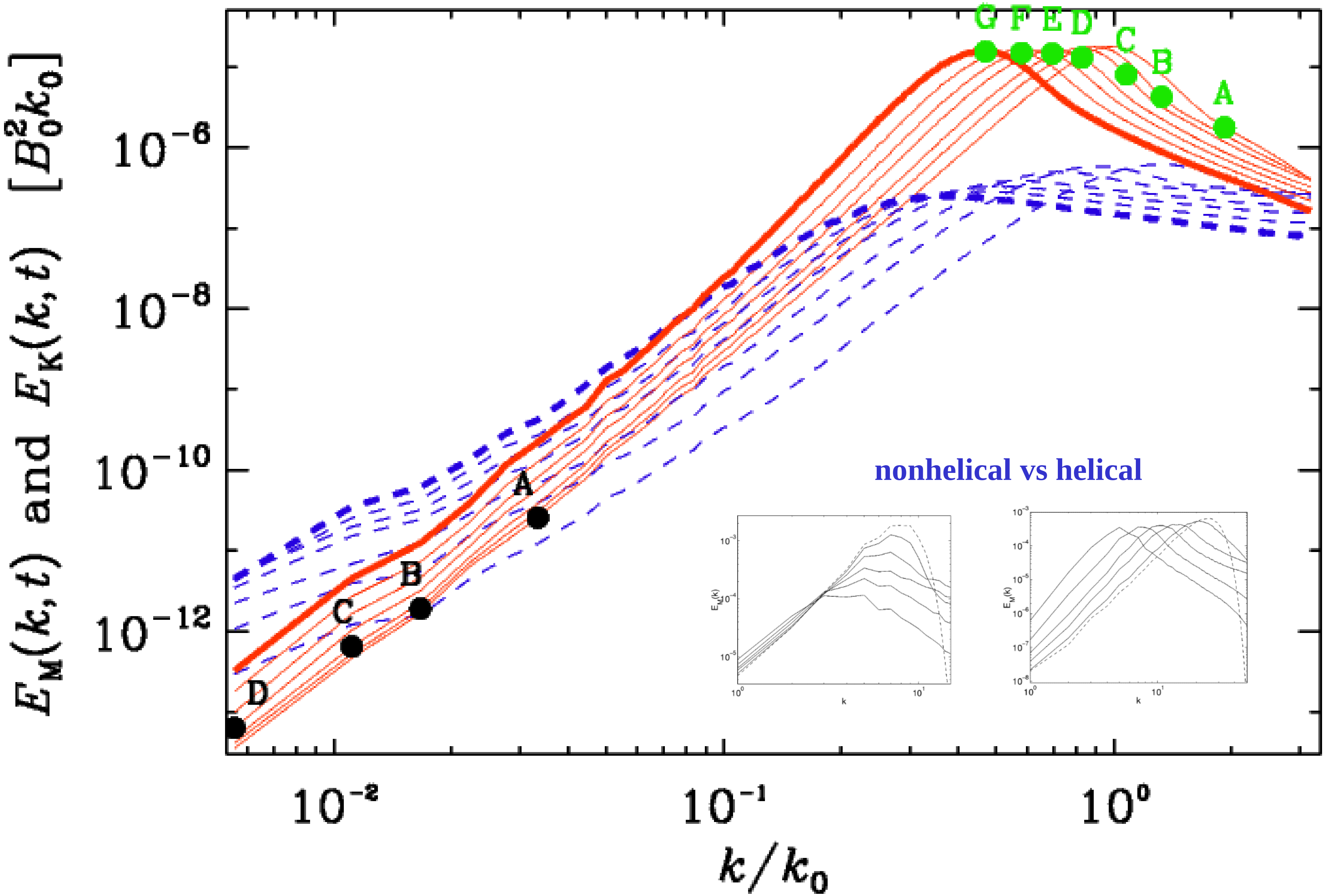

Correspondence of spectra

$$\left(\partial_{\bar{t}}^2 - c^2\nabla^2\right) h_{ij}(\boldsymbol{x},\bar{t}) = 6\,T_{ij}^{\mathrm{TT}}(\boldsymbol{x},\bar{t})/\bar{t}$$

$$T_{ij} = (p+\rho)\,\gamma^2 u_i u_j - B_i B_j + (p + \boldsymbol{B}^2/2)\delta_{ij}$$

- If spectral slope of B is -5/3, then
- Spectral slope of B^2 is -5/3-2 = -11/3
- But for slope 4, we don't get 4-2 = 2, but 0.

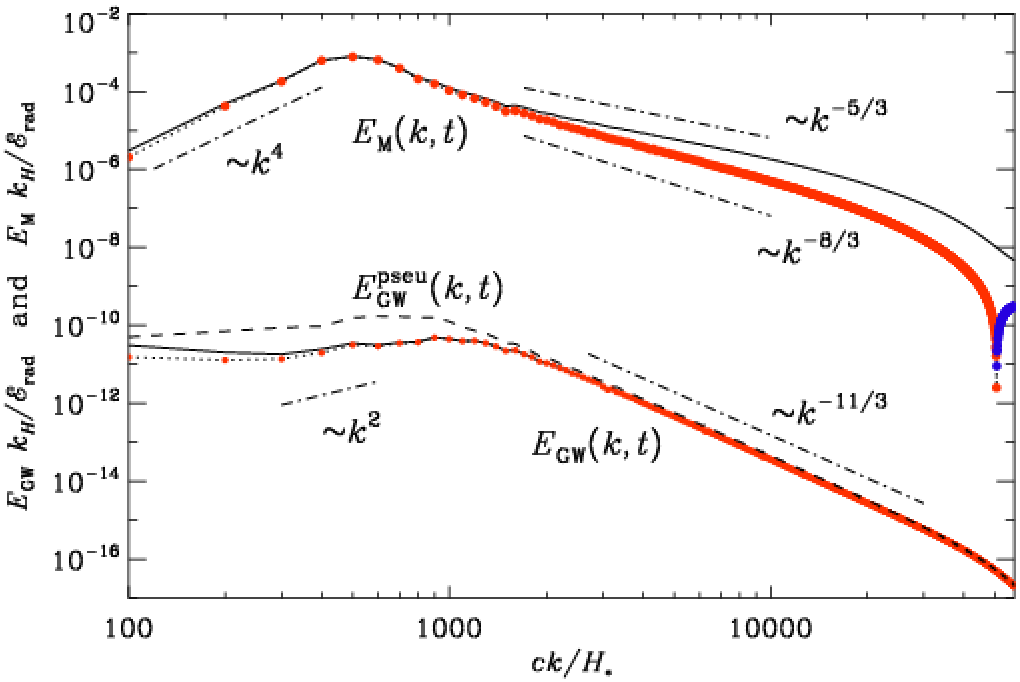

Spectra of the source

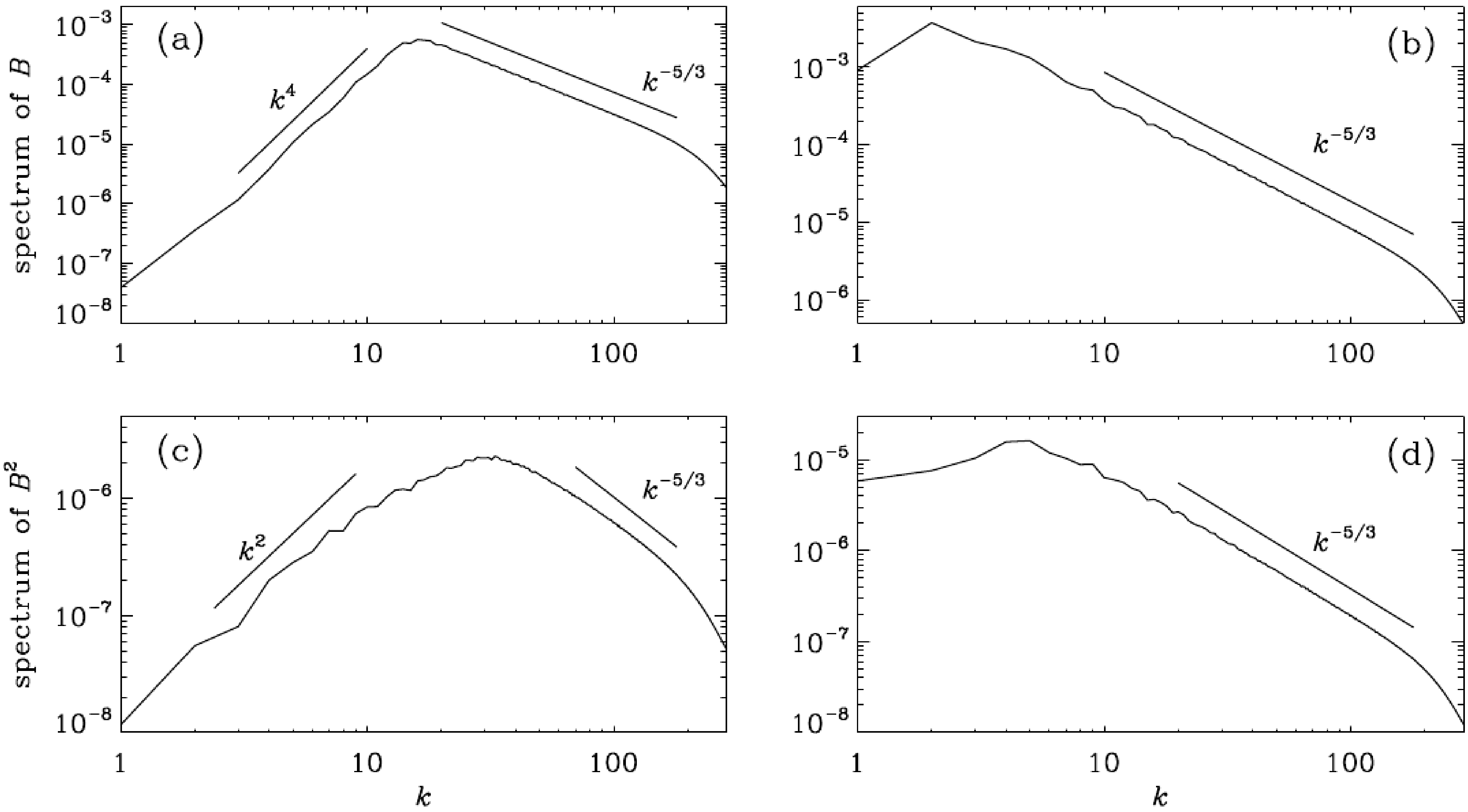

Experiments with scalar fields s

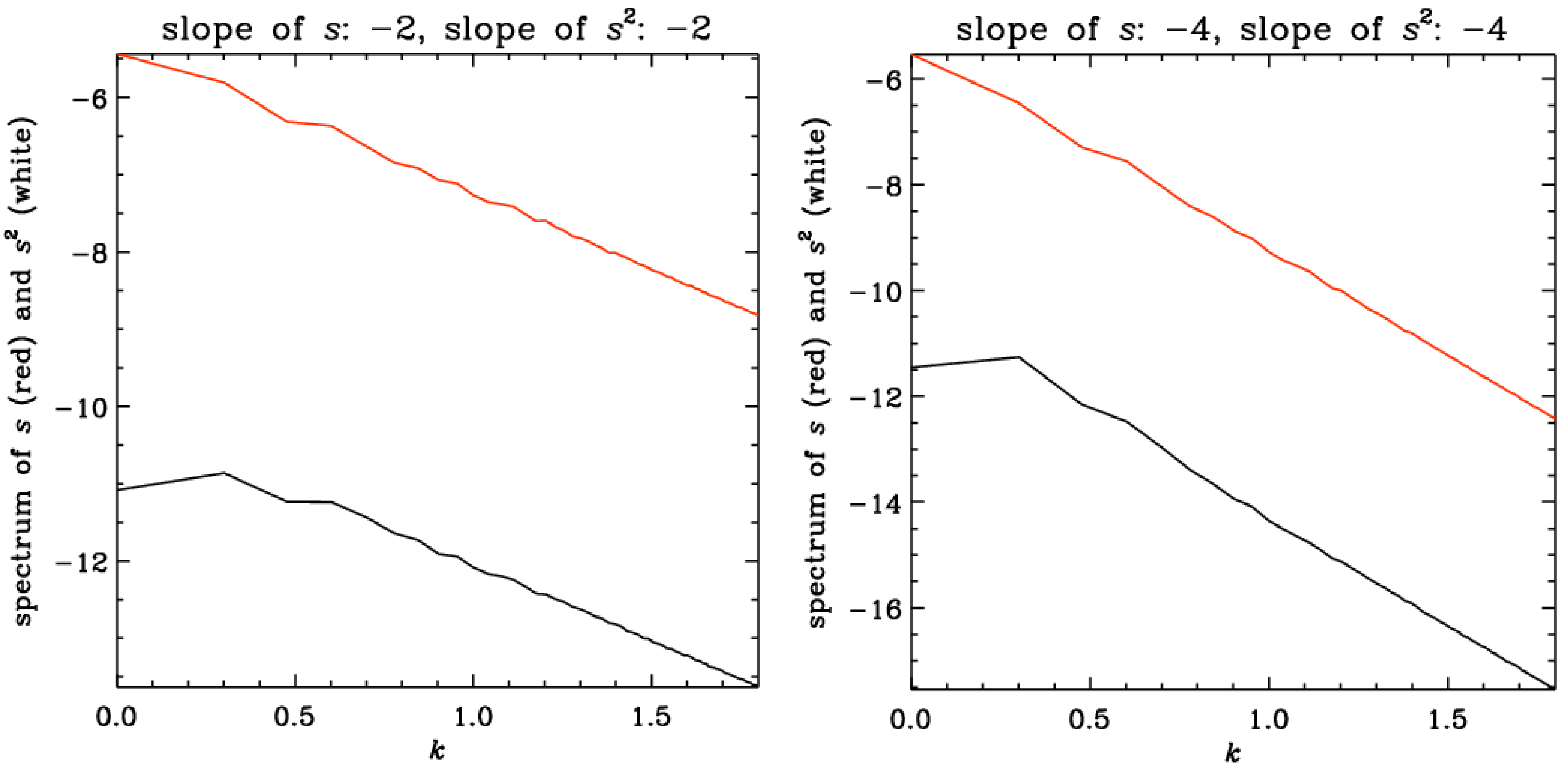

- Spectrum of source agrees with spectrum of d^2h/dt^2
- Spectrum of d^2h/dt^2 agrees with that of $k\,dh/dt$
- Therefore, spectrum of h is k^{-2} times that of source

Same for positive slopes

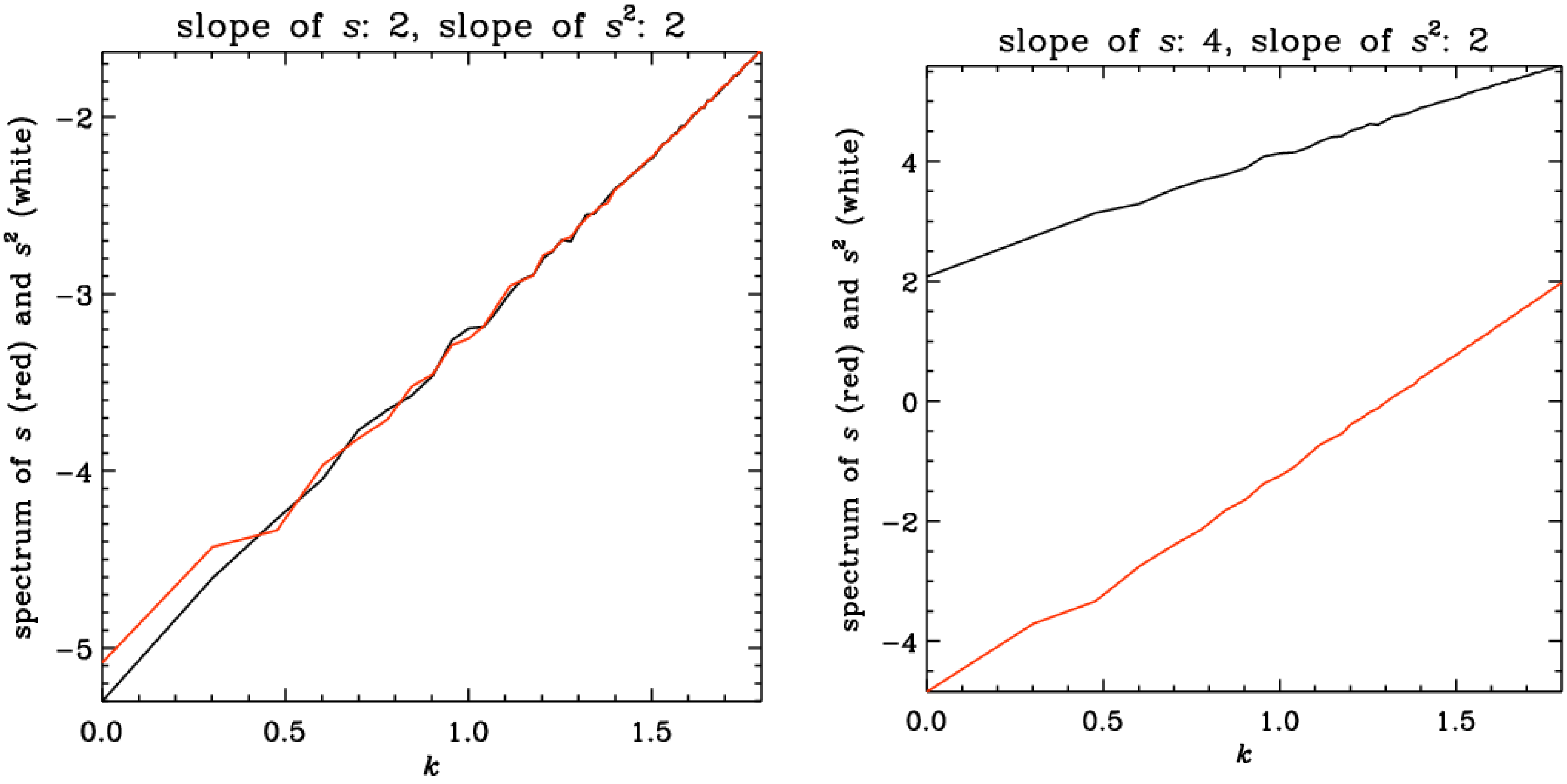

- k^2 spectrum is that of while noise (shell integrated!)
- Its square is also that of white noise
- Even a bluer spectrum becomes white again

Intermediate cases

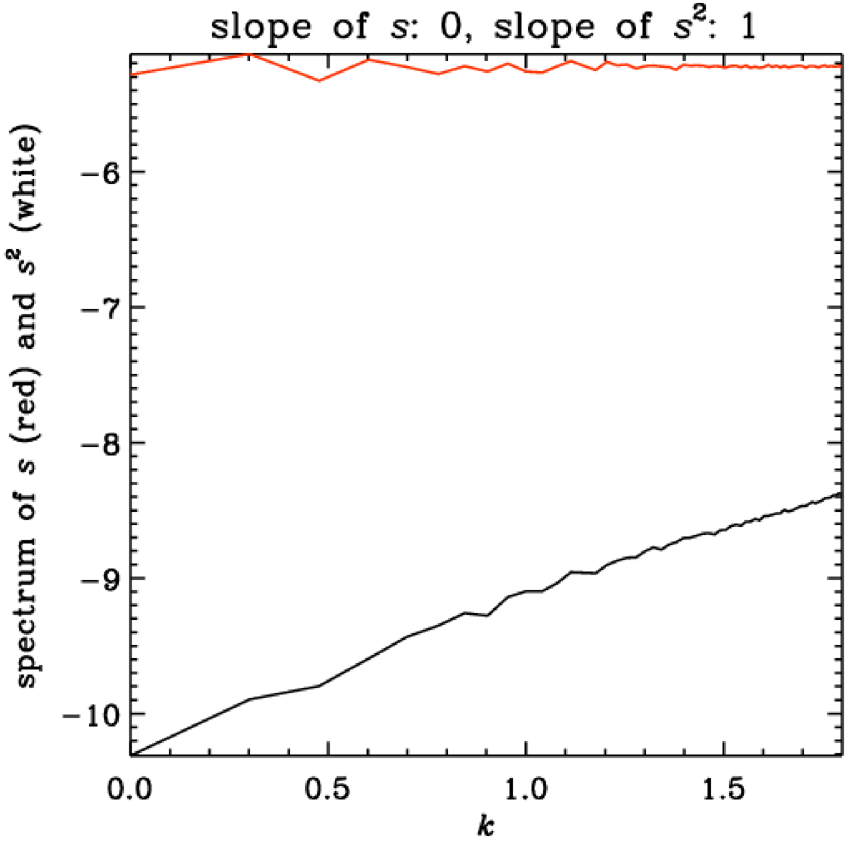

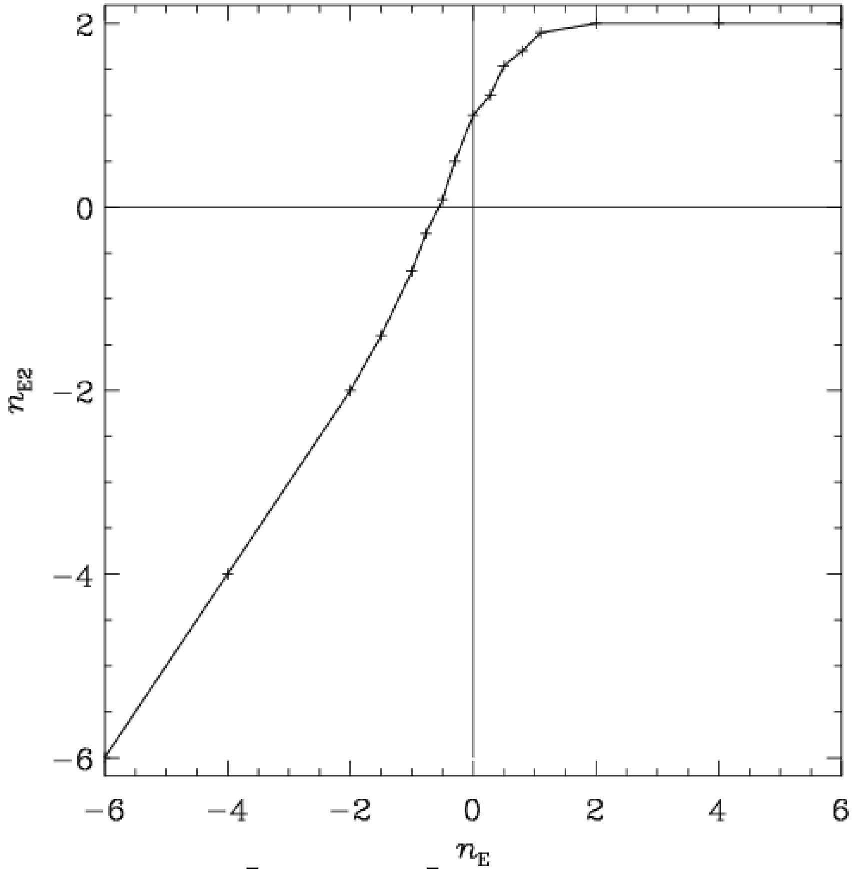

- For slopes btw -2 and 2: more complicated
- For red spectra (negative slope): same
- For blue spectra (steeper than 2): always 2 (white)

Energy per linear & logarithmic k interval

slope of	naive exp	new	Kol	Gol
E_{M}	4	—	$-5/3$	$-11/3$
$E_{\mathrm{GW}} \propto S_{\dot{h}}$	2	0	$-11/3$	$-17/3$
$\Omega_{\mathrm{GW}} \propto k S_{\dot{h}}$	3	1	$-8/3$	$-14/3$
S_h	0	-2	$-17/3$	$-23/3$
$k S_h$	1	-1	$-14/3$	$-20/3$
h_c	$1/2$	$-1/2$	$-7/3$	$-10/3$

- Different sign of slope of characteristic strain!

GW energy & strain spectra

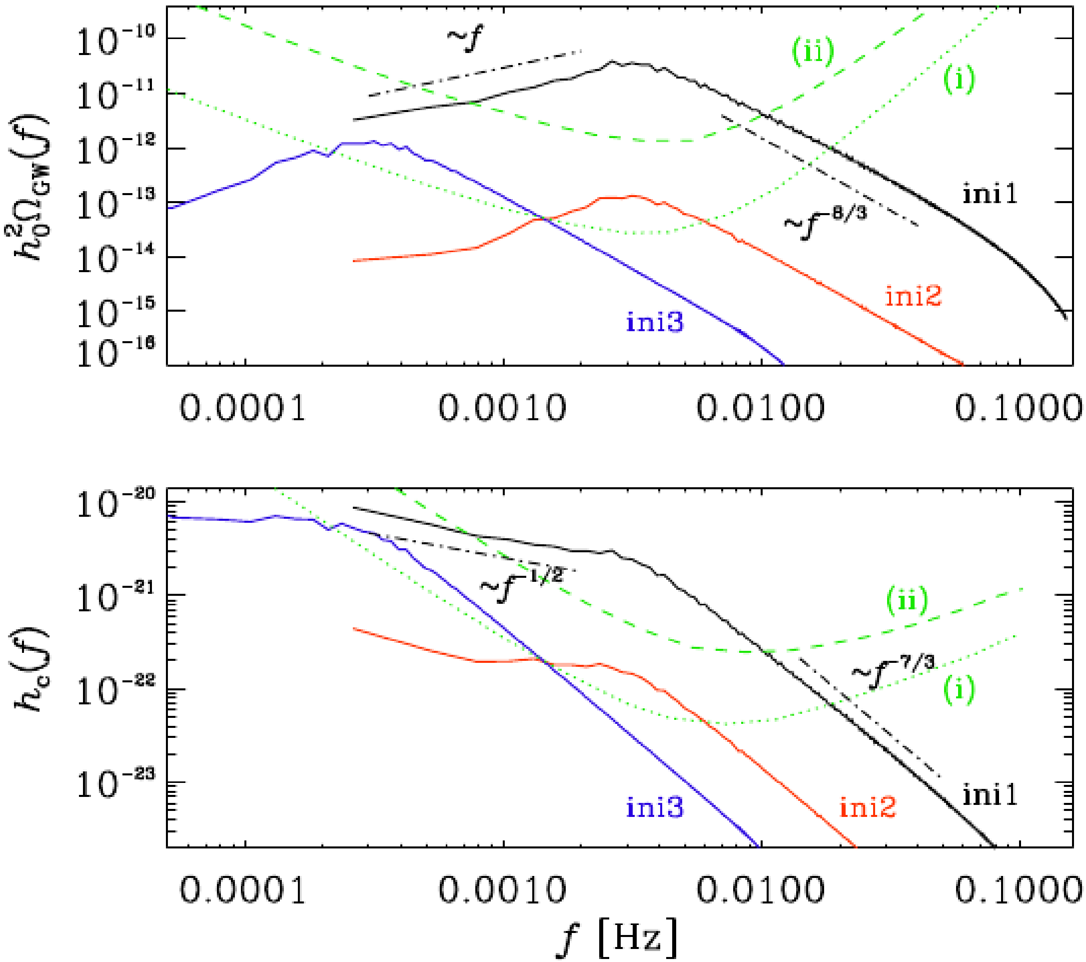

slope of	exp	new	Kol
E_{M}	4	—	$-5/3$
$E_{\mathrm{GW}} \propto S_{\dot{h}}$	2	0	$-11/3$
$\Omega_{\mathrm{GW}} \propto kS_{\dot{h}}$	3	1	$-8/3$
S_h	0	-2	$-17/3$
kS_h	1	-1	$-14/3$
h_c	$1/2$	$-1/2$	$-7/3$

- confirm also -8/3 and -7/3

PHYSICAL REVIEW D **76,** 083002 (2007)

Spectrum of gravitational radiation from primordial turbulence

Grigol Gogoberidze,[1,2,*] Tina Kahniashvili,[3,2,†] and Arthur Kosowsky[4,‡]

[1]*Centre for Plasma Astrophysics, K.U. Leuven, Celestijnenlaan 200B, 3001 Leuven, Belgium*
[2]*National Abastumani Astrophysical Observatory, 2A Kazbegi Ave, GE-0160 Tbilisi, Georgia*
[3]*Center for Cosmology and Particle Physics, New York University, 4 Washington Plaza, New York, New York 10003, USA*
[4]*Department of Physics and Astronomy, University of Pittsburgh, 3941 O'Hara Street, Pittsburgh, Pennsylvania 15260, USA*

(Received 4 May 2007; published 5 October 2007)

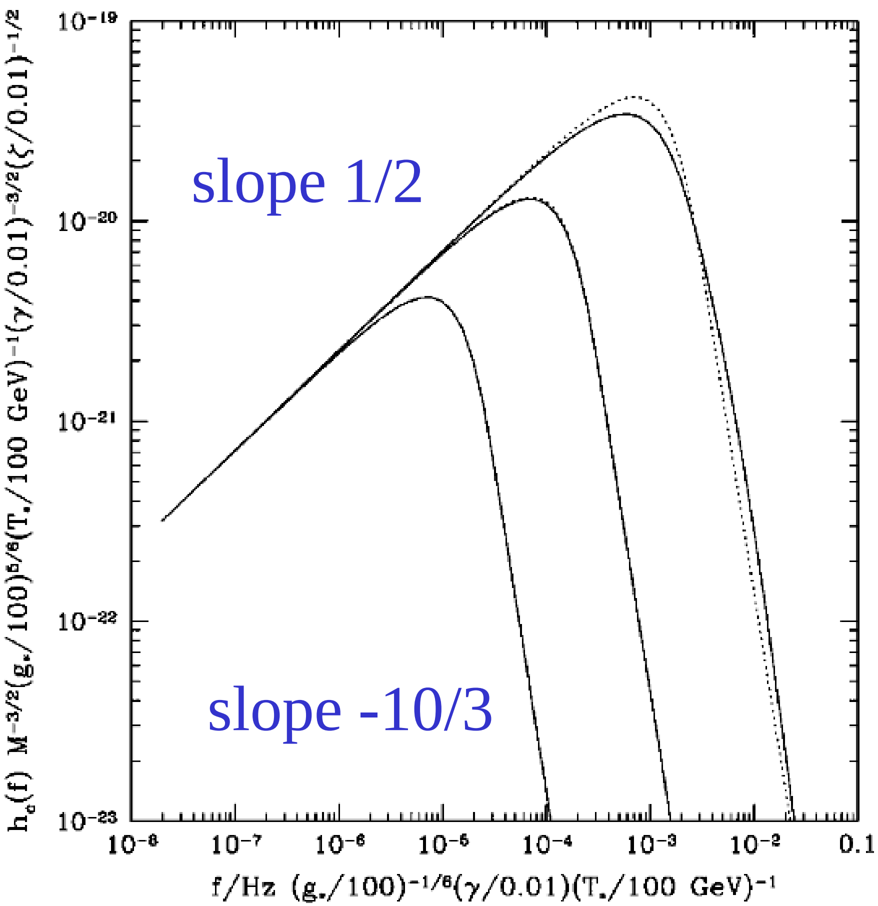

- Lighthill approx.
- $h(f) \sim 3\times10^{-20}$
- +1/2 slope, not -1/2
- -10/3, not -7/3

slope of	exp	new	Kol	Gol
$E_{\rm M}$	4	—	$-5/3$	$-11/3$
$E_{\rm GW} \propto S_h$	2	0	$-11/3$	$-17/3$
$\Omega_{\rm GW} \propto kS_h$	3	1	$-8/3$	$-14/3$
S_h	0	-2	$-17/3$	$-23/3$
kS_h	1	-1	$-14/3$	$-20/3$
h_c	1/2	$-1/2$	$-7/3$	$-10/3$

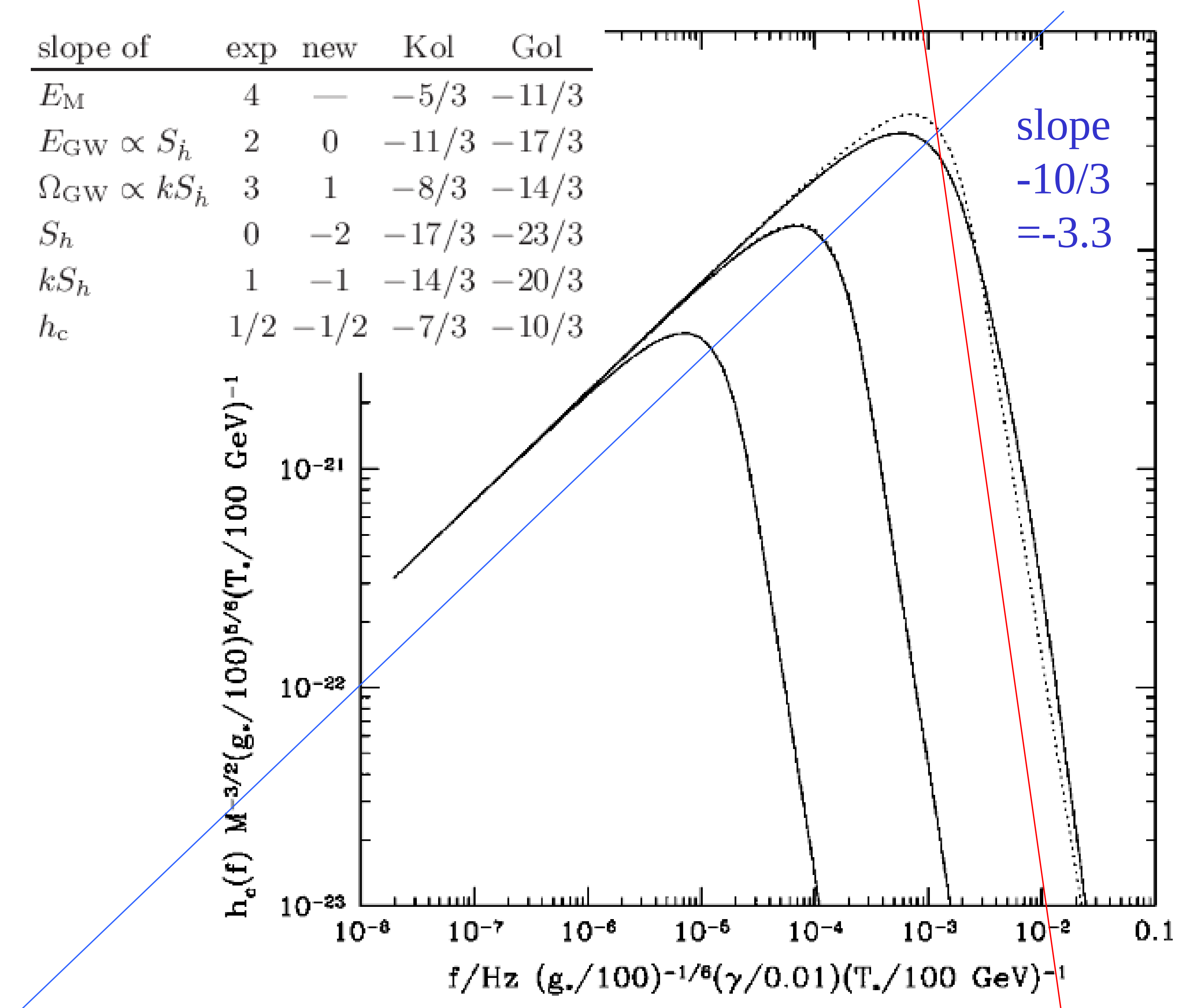

PHYSICAL REVIEW D **78,** 123006 (2008)

Gravitational radiation from primordial helical inverse cascade magnetohydrodynamic turbulence

Tina Kahniashvili,[1,2,3] Leonardo Campanelli,[4,5] Grigol Gogoberidze,[1,3,6] Yurii Maravin,[1] and Bharat Ratra[1]
[1]*Department of Physics, Kansas State University, 116 Cardwell Hall, Manhattan, Kansas 66506, USA*
[2]*Department of Physics, Laurentian University, Ramsey Lake Road, Sudbury, ON P3E 2C6, Canada*
[3]*National Astrophysical Observatory, Ilia Chavchavadze State University, 2A Kazbegi Ave, Tbilisi, GE-0160, Georgia*
[4]*Dipartimento di Fisica, Università di Bari, I-70126 Bari, Italy*
[5]*INFN - Sezione di Bari, I-70126 Bari, Italy*
[6]*Centre for Plasma Astrophysics, K.U. Leuven, Celestijnenlaan 200B, 3001 Leuven, Belgium*
(Received 10 September 2008; published 16 December 2008)

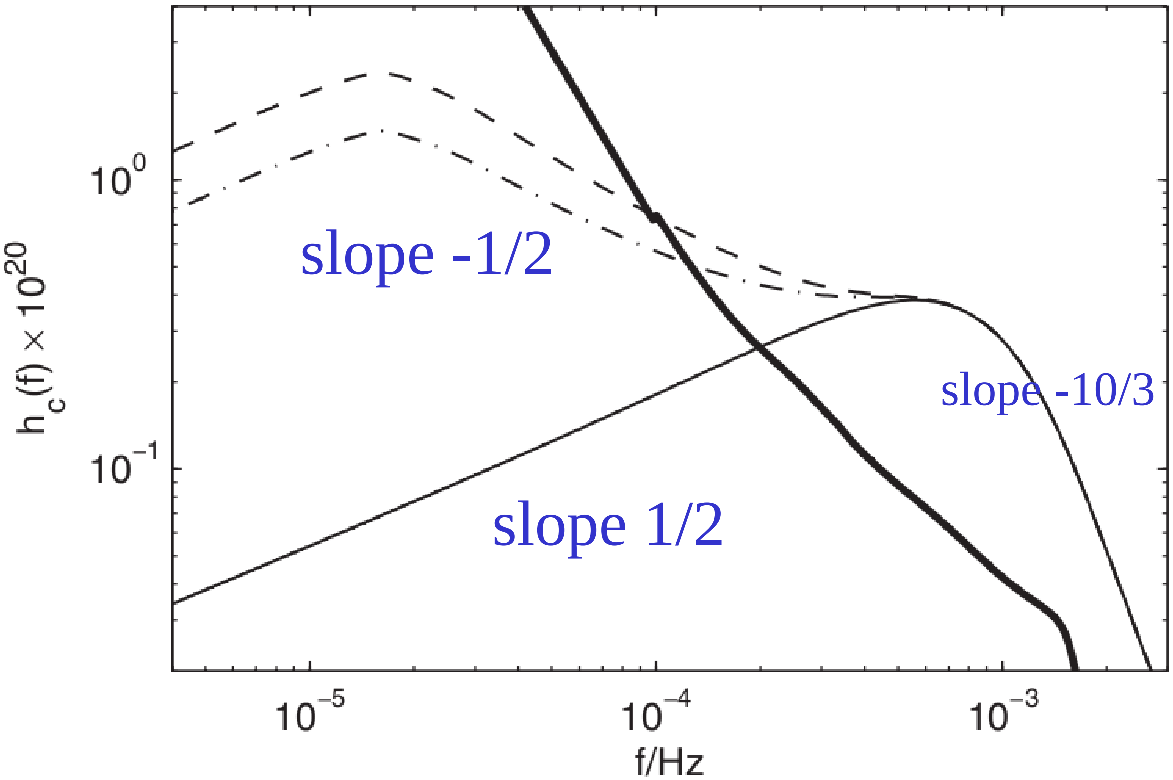

- Inverse cascade
- Duration of source
- Peak moves left
- Now negative slope
- Agreement with simulations?
- Still -10/3, not -7/3

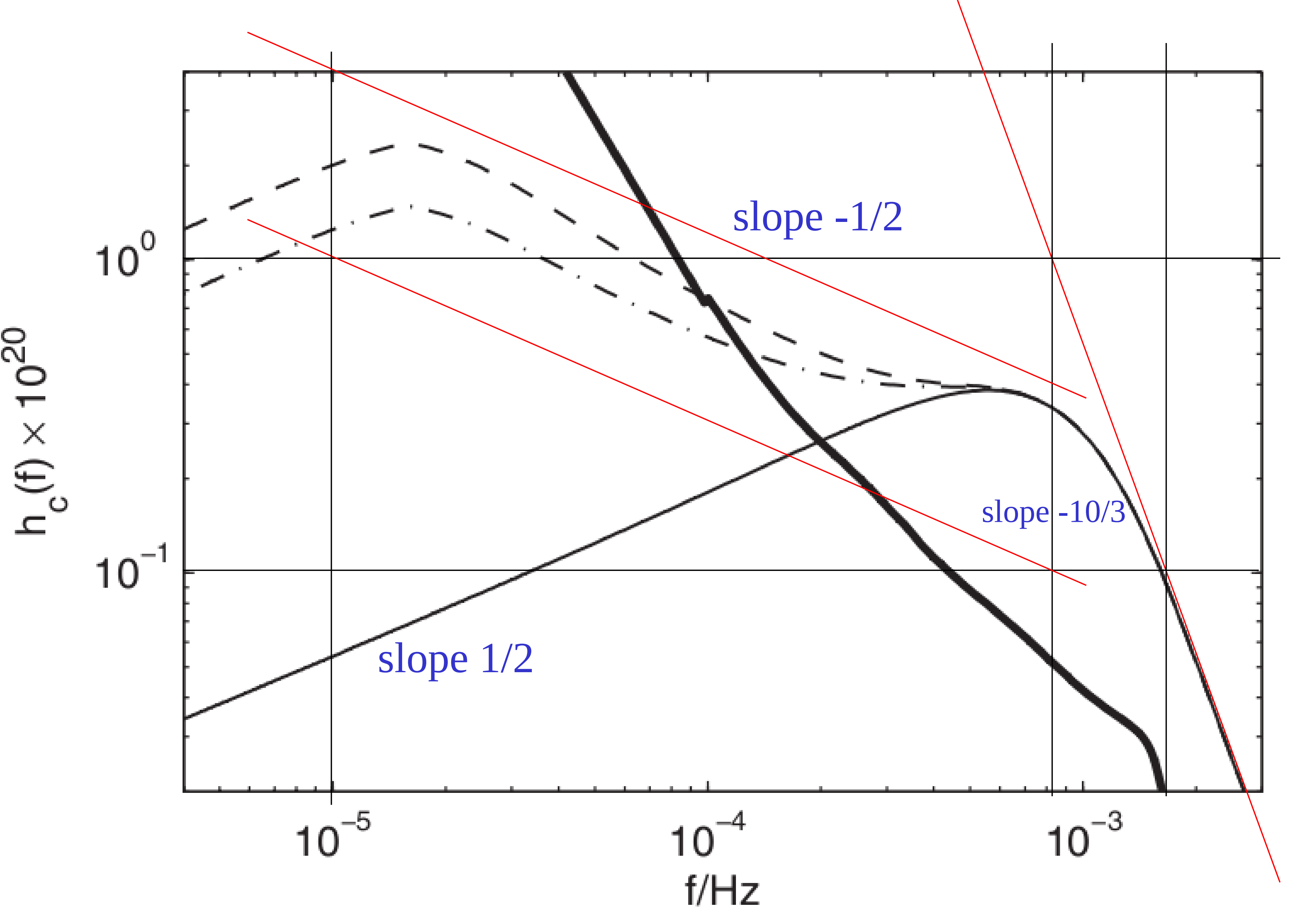

slope -1/2
slope -10/3
slope 1/2
10^0
10^{-1}
$h_c(f) \times 10^{20}$
10^{-5}
10^{-4}
10^{-3}
f/Hz

Effect of inv cascade on GW spectrum

- Significant transfer to the left
- Yet no increase of GW energy
- Was determined by maximum

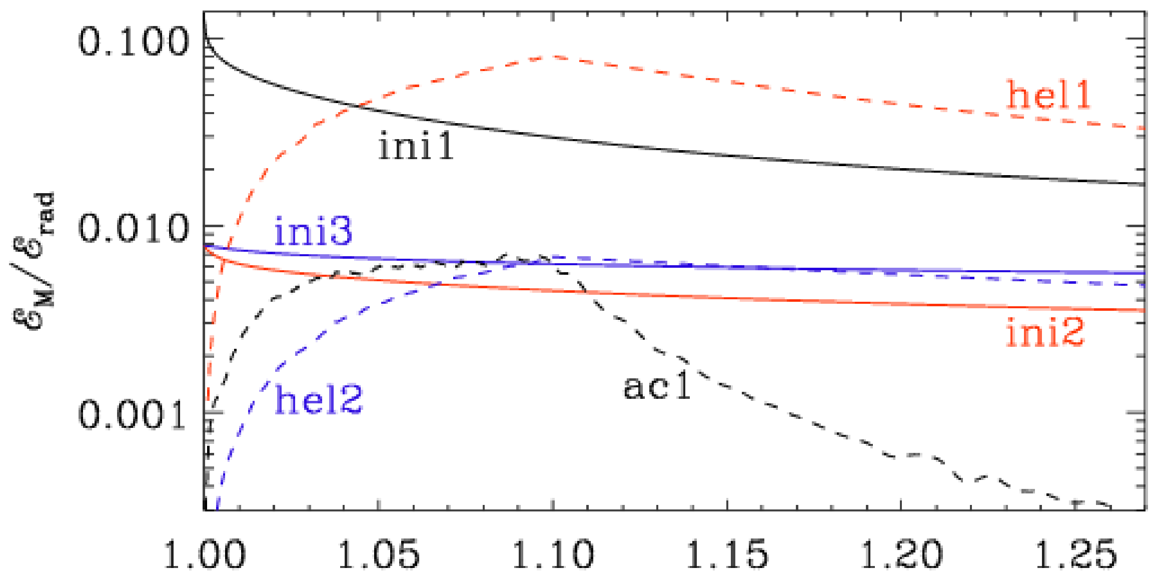

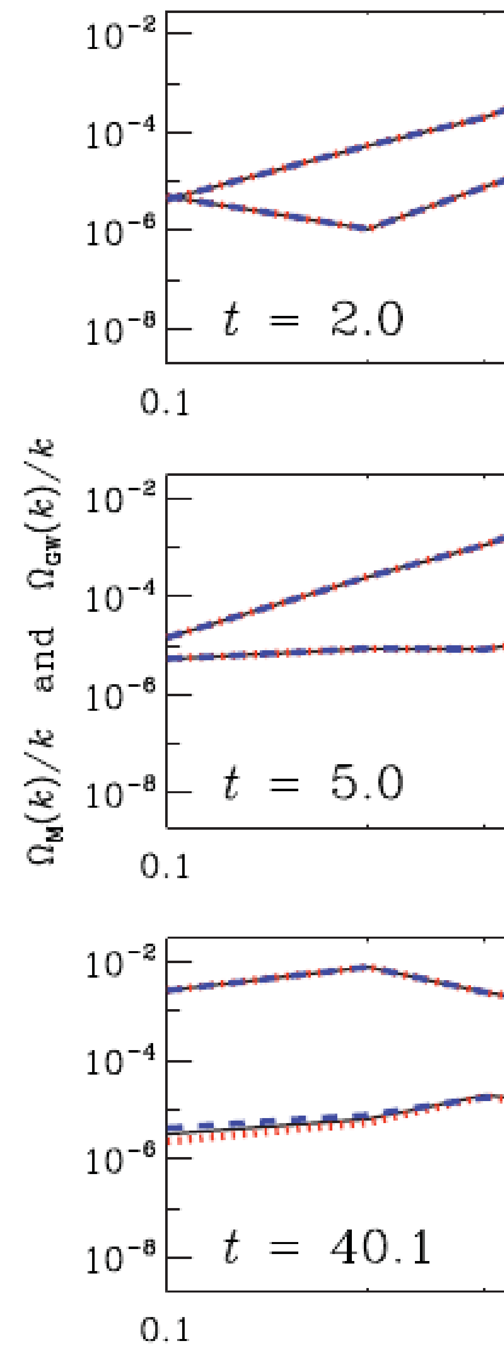

from Alberto's talk

- Relation between peak and GW energy

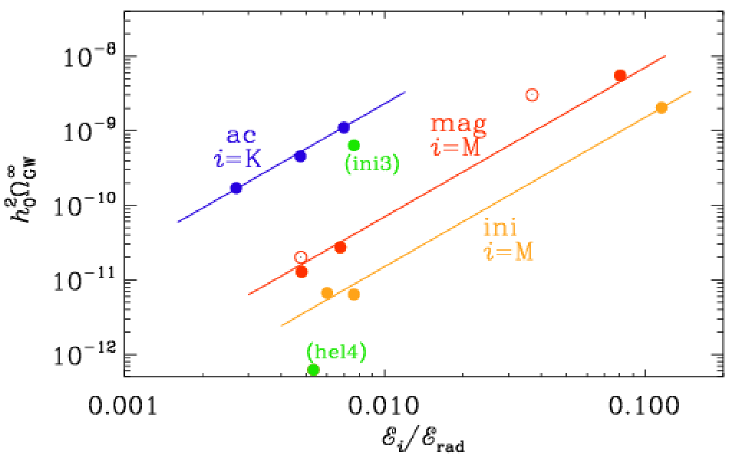

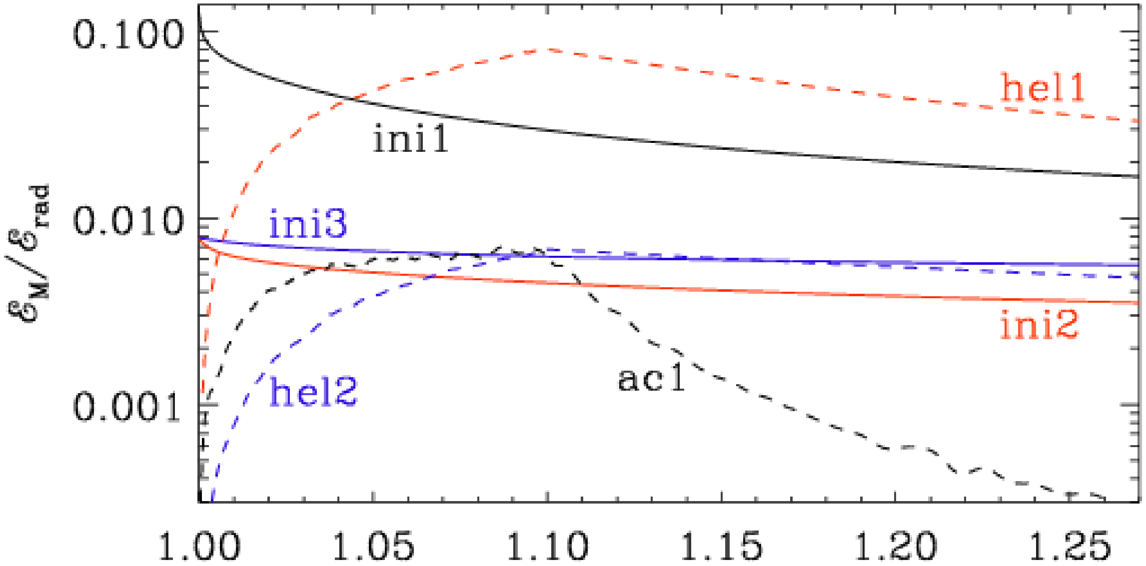

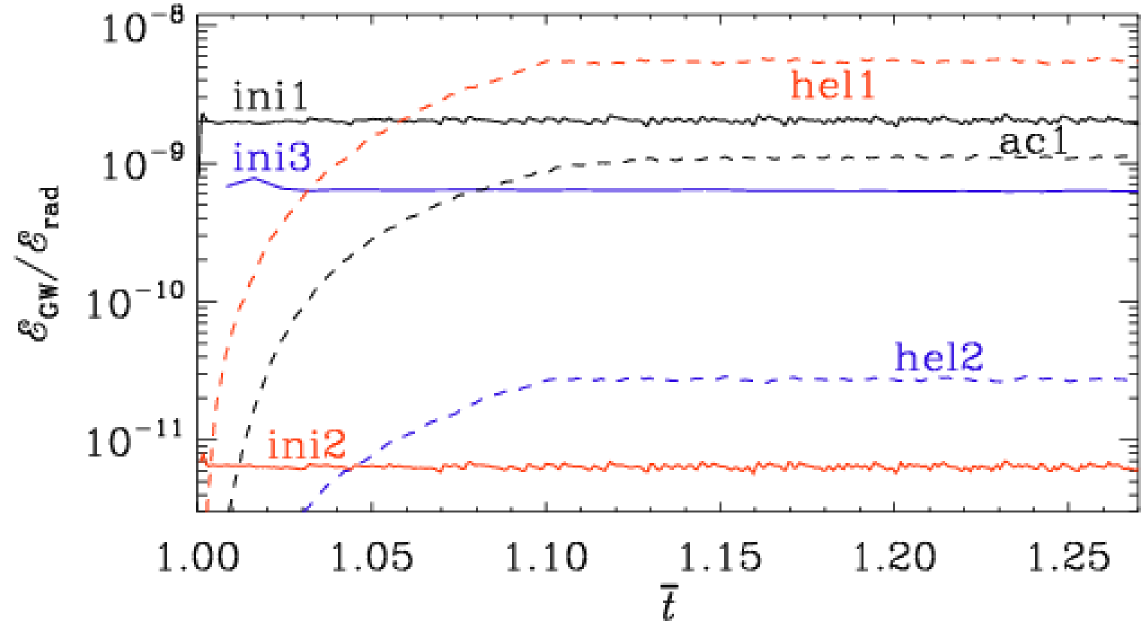

Non-abrupt end of driving

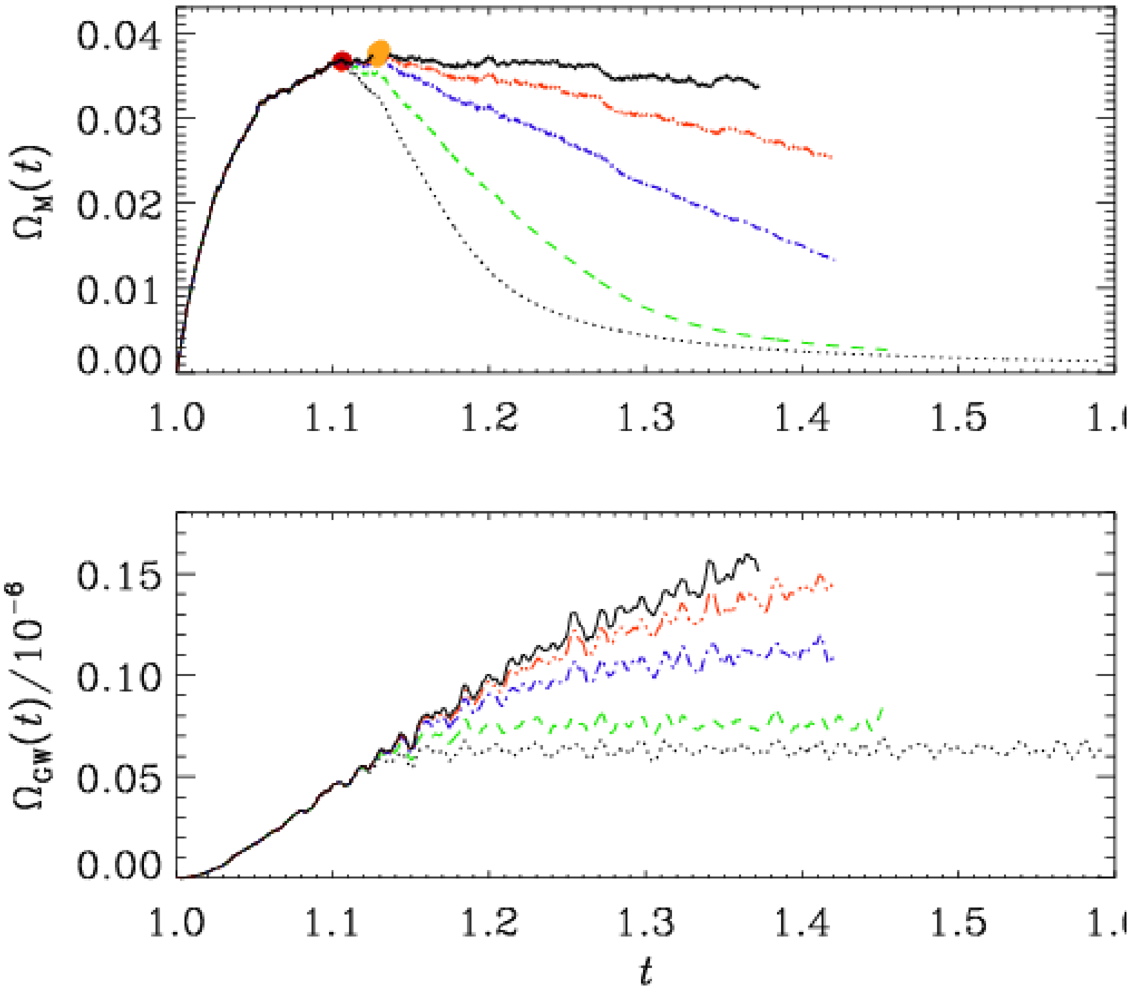

- Larger GW energy from graceful exit
- GW energy can be ~3x larger
- To understand slope-amplitude relation

Longer runs

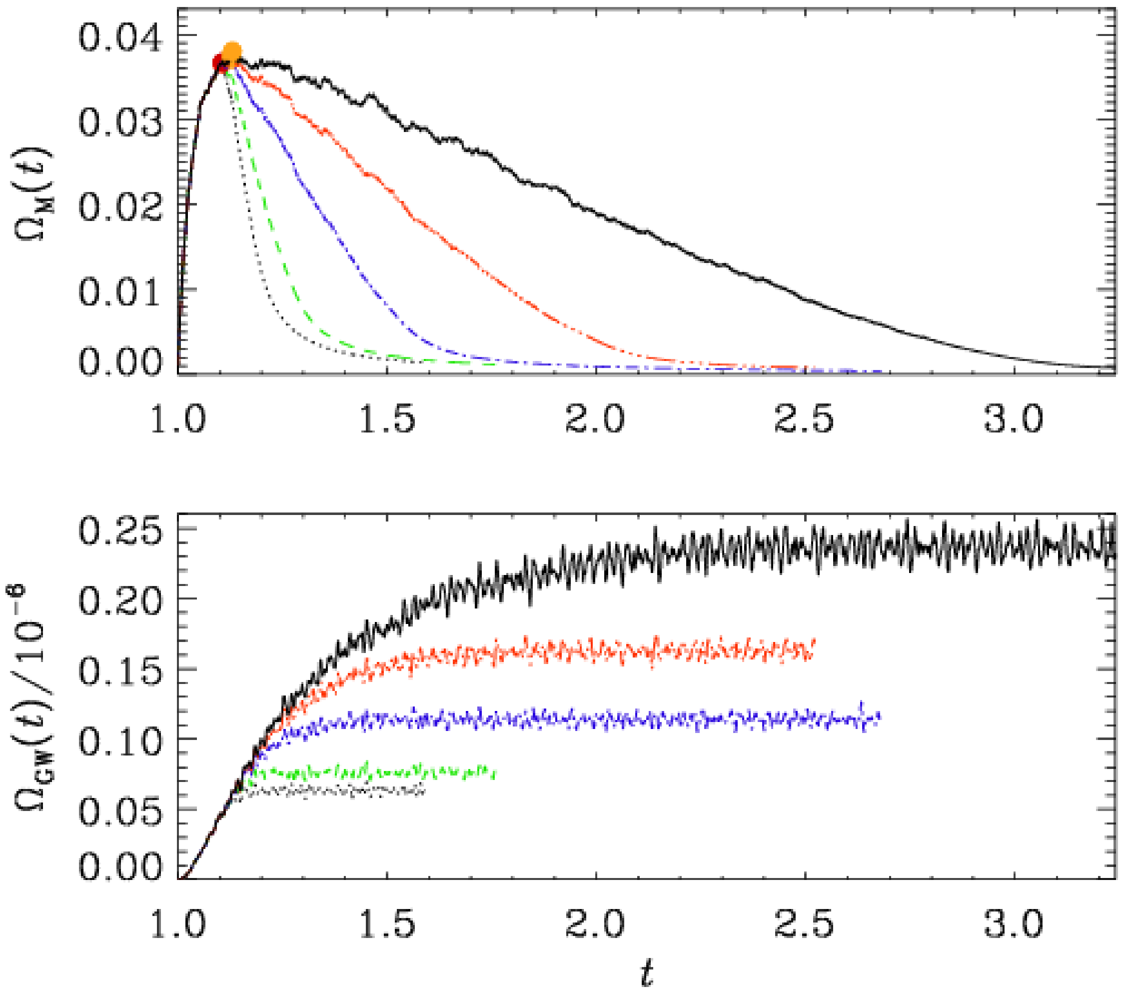

- Indeed: GW energy can be ~3x larger
- stops growing when Ω_{GW} drops below certain value
- About 20% of maximum?

Spectra from driven case

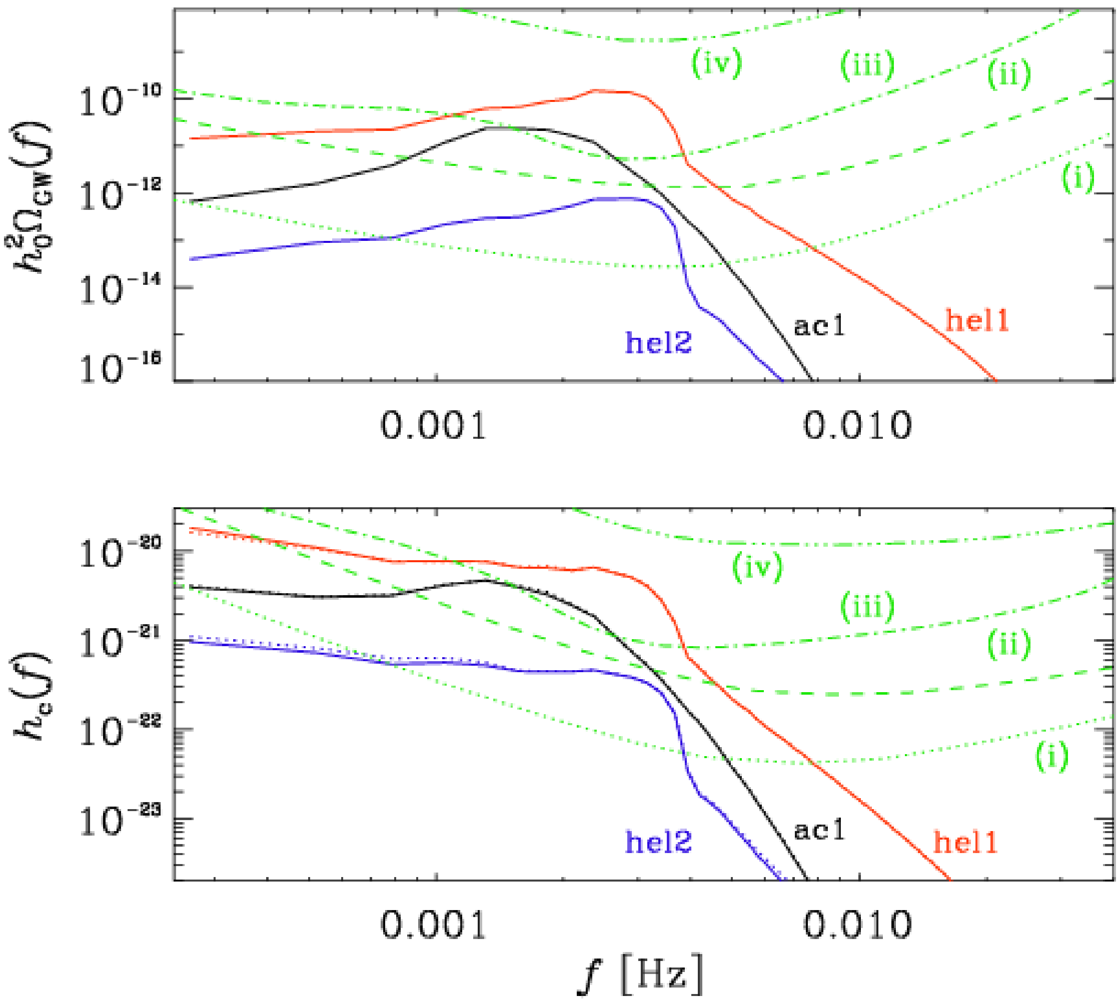

- Sharp drop
- Long subinertial range

Irrotational ←→ Vortical

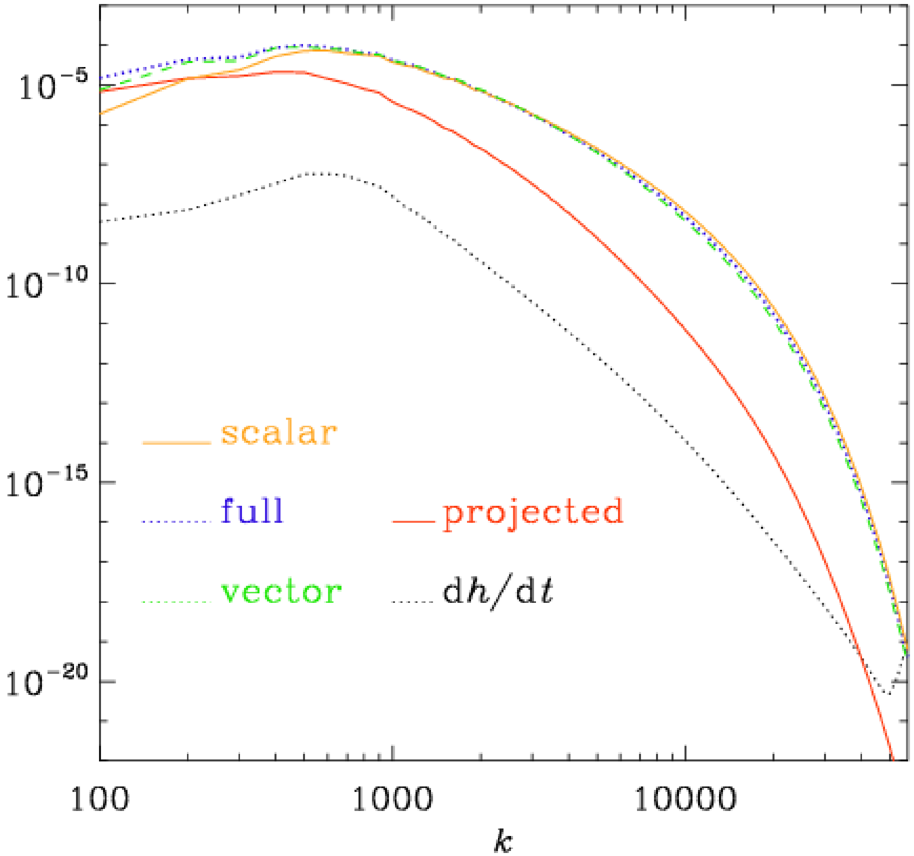

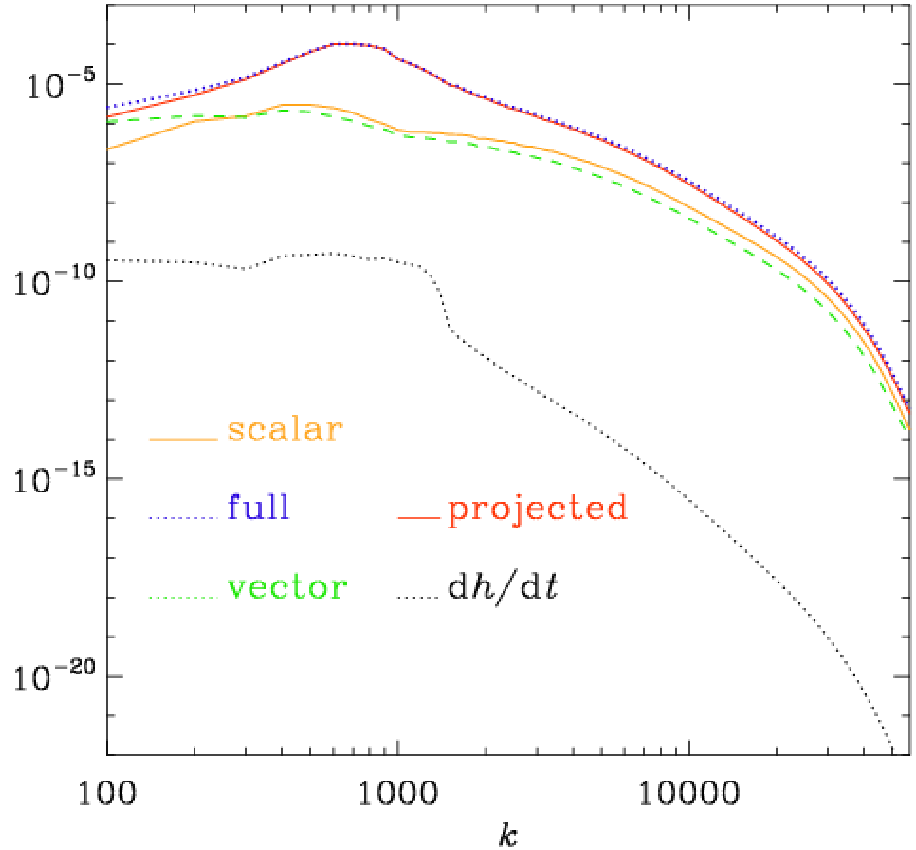

- Irrotational: scalar & vector dominant
- Vortical: subdominant, so full~projected!

Irrotational: no dynamo, & hardly any vorticity

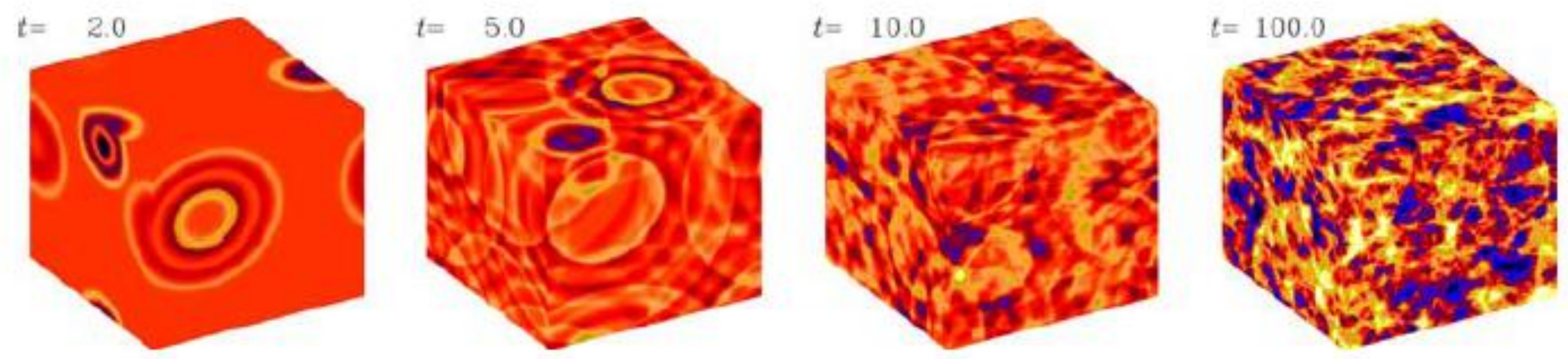

$$\frac{\partial \mathbf{B}}{\partial t} = \nabla \times (\mathbf{u} \times \mathbf{B}) + \eta \nabla^2 \mathbf{B}$$

$$\frac{\partial \boldsymbol{\omega}}{\partial t} = \nabla \times (\mathbf{u} \times \boldsymbol{\omega}) + \nu \nabla^2 \boldsymbol{\omega} + \nabla \times (\mathbf{S} \cdot \nabla \ln \rho)$$

Table 1. Results for the normalized vorticity, $\omega_{\rm rms}/(u_{\rm rms}\, k_{\rm peak})$, as a function of Re and resolution. The durations of the runs vary between $N_{\rm turn} =$ 16 and 250 turnover times, and ν varies between 10^{-3} and 5×10^{-5}. For the high resolution run with 512^3 mesh points and $\nu = 5 \times 10^{-5}$, we have $N_{\rm turn} = 59$ turnover times.

Re	512^3	256^3	128^3
50	$1.4 + \times 10^{-3}$	8.7×10^{-3}	
25		1.1×10^{-2}	2.9×10^{-3}
12		1.6×10^{-2}	2.0×10^{-3}
4		7.6×10^{-3}	1.5×10^{-3}

GW and vorticity

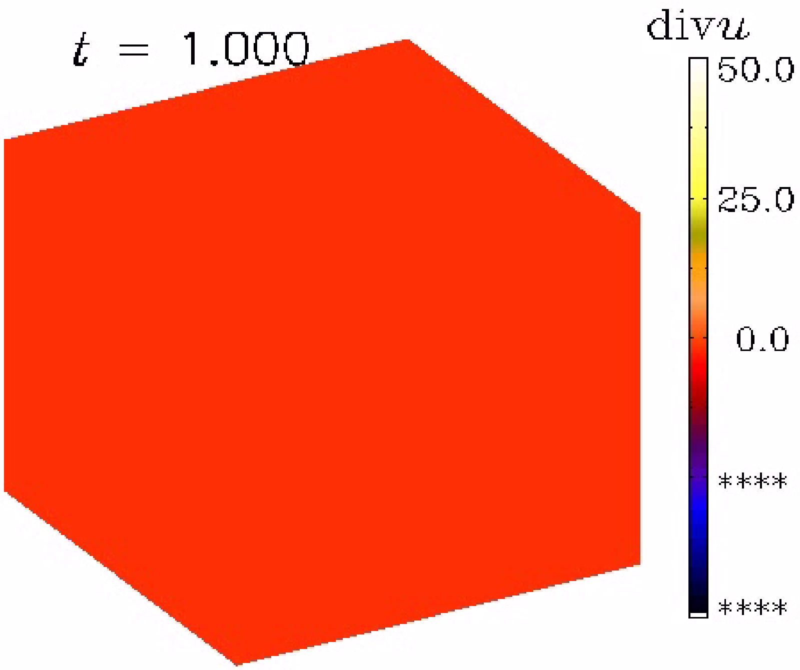

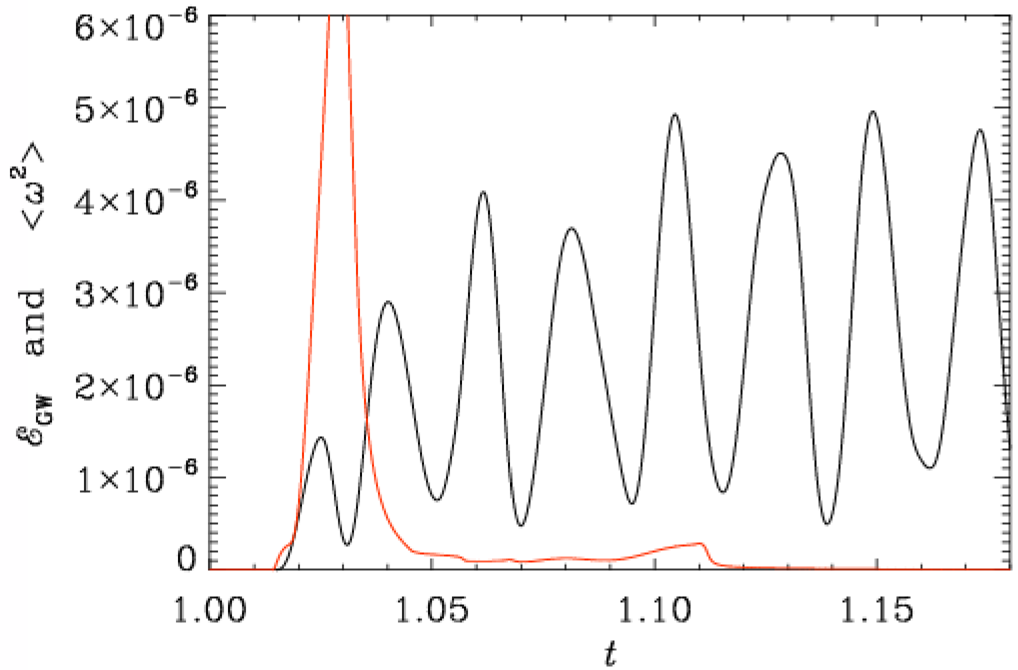

- Vorticity from obique shocks
- GW perhaps consequence of vorticity

Simple example

$$\left(\partial_t^2 + 3H\partial_t - c^2\nabla^2\right) h_{ij}(\boldsymbol{x},t) = \frac{16\pi G}{c^2} T_{ij}^{\mathrm{TT}}(\boldsymbol{x},t)$$

$$T_{ij}(\boldsymbol{x},t) = \left(p/c^2 + \rho\right)\gamma^2 u_i u_j - B_i B_j + (\boldsymbol{B}^2/2 + p)\delta_{ij}$$

Example

$$\boldsymbol{B} = \begin{pmatrix} 0 \\ \sigma \sin kx \\ \cos kx \end{pmatrix} \longrightarrow \boldsymbol{\nabla} \times \boldsymbol{B} = \begin{pmatrix} \partial_x \\ 0 \\ 0 \end{pmatrix} \times \begin{pmatrix} 0 \\ \sin kx \\ \cos kx \end{pmatrix} = k \begin{pmatrix} 0 \\ \sin kx \\ \cos kx \end{pmatrix} = k\boldsymbol{B}$$

Traceless-transverse

$$T_{ij}(x) = \mathcal{E}_{\mathrm{M}} \begin{pmatrix} 0 & 0 & 0 \\ 0 & -\cos 2kx & \sigma \sin 2kx \\ 0 & \sigma \sin 2kx & \cos 2kx \end{pmatrix}$$

Early examples

Projection operator $\hat{T}_{ij}^{\mathrm{TT}}(\boldsymbol{k},t) = (P_{il}P_{jm} - \frac{1}{2}P_{ij}P_{lm})\hat{T}_{lm}(\boldsymbol{k},t)$

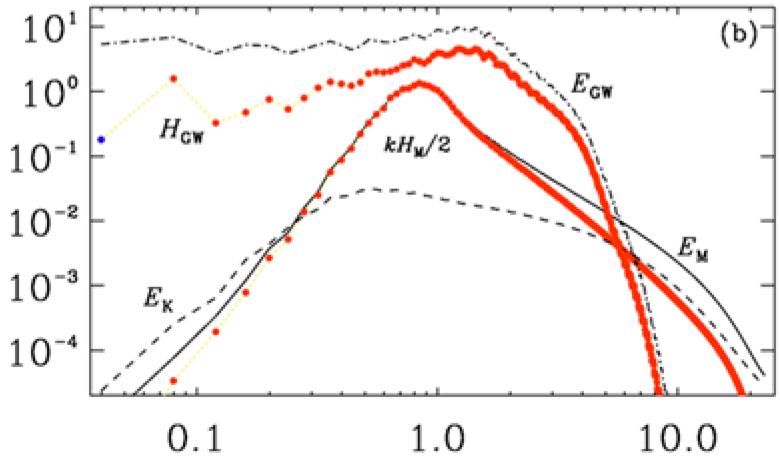

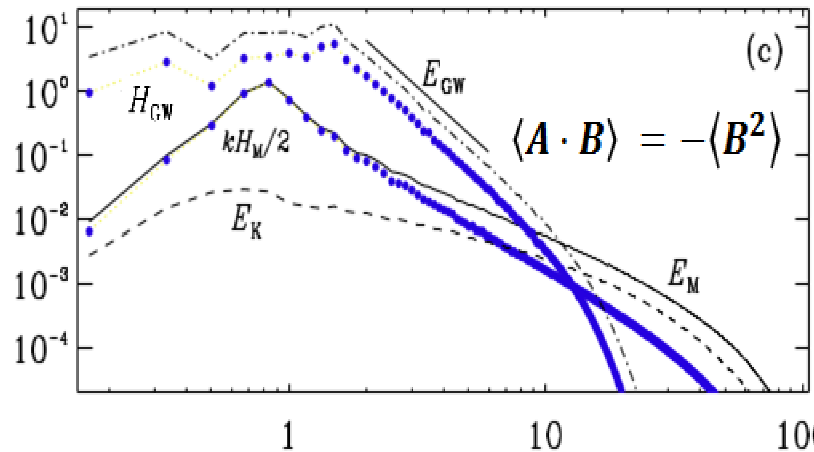

- Magnetic energy spectrum $\int E_{\mathrm{M}}(k,t)\,dk = \langle \boldsymbol{B}^2\rangle/2$
- Positive helicity (red), negative (blue)
- GW energy spectra

Conclusion

- Pencil Code: GW advanced exactly
- For $E(k) \sim k^{-5/3}$ we get $\Omega(k) \sim k^{-8/3}$ and $h_c(k) \sim k^{-7/3}$
  - not -14/3 and -10/3
- but $E(k) \sim k^4$ leads to $\Omega(k) \sim k$ and $h_c(k) \sim k^{-1/2}$
  - not 3 and +1/2
- Vortical turbulence: vector & scalar modes weak
- Irrotational (acoustic) turbulence: they are strong, especially at small scales
  - GW generation coincides with onset of vorticity generation